SYNTHESIS OF ZWITTERIONIC CYANINE DYES

FOR USE IN PROTEOMICS

by

Mark Galen Epstein

A thesis submitted in partial fulfillment
of the requirements for the degree

of

Master of Science

in

Chemistry

MONTANA STATE UNIVERSITY
Bozeman, Montana

November 2012

APPROVAL

of a thesis submitted by

Mark Galen Epstein

This thesis has been read by each member of the thesis committee and has been found to be satisfactory regarding content, English usage, format, citation, bibliographic style, and consistency and is ready for submission to The Graduate School.

Dr. Paul A. Grieco

Approved for the Department of Chemistry

Dr. Mary Cloninger

Approved for The Graduate School

Dr. Ronald W. Larsen

STATEMENT OF PERMISSION TO USE

In presenting this thesis in partial fulfillment of the requirements for a master's degree at Montana State University, I agree that the Library shall make it available to borrowers under rules of the Library.

If I have indicated my intention to copyright this thesis by including a copyright notice page, copying is allowable only for scholarly purposes, consistent with "fair use" as prescribed in the U.S. Copyright Law. Requests for permission for extended quotation from or reproduction of this thesis in whole or in parts may be granted only by the copyright holder.

Mark Galen Epstein

November 2012

DEDICATION

To Dennis R. Epstein and Linda J. Brewer, who have always supported and encouraged me to find my own adventure.

TABLE OF CONTENTS

LIST OF TABLES

Table Page

LIST OF FIGURES

LIST OF SCHEMES

Scheme Page

ABSTRACT

The CyDye family of fluorescent dyes are the tools currently in use today for applications in two dimensional difference gel electrophoresis (2D-DIGE) techniques. The lysine labeling CyDyes are limited by problems with over labeling resulting in protein precipitation and isoelectric point (pI) drift at high pH's. These limitations have been addressed by a family of highly water soluble and pI balancing zwitterionic BODIPY dyes, which were previously synthesized in the Grieco group. The absorbance maxima of the BODIPY fluorophores were tuned through extension of the π system to produce a three color, spectrally resolved dye set. However the fluorescence of the green emitting BOPIDY suffered at pH's less than 3.5 and greater than 11, while the red emitting BODIPY was susceptible to Michael addition changing its emission profile. To address the limitations of the BODIPY family of dyes, a new family of zwitterionic 2D-DIGE dyes based on the established CyDye fluorophores have been synthesized. A complete three dye zwitterionic minimal labeling set which features a cysteic acid motif, titratable amine functionality and an NHS activated ester group reactive towards lysine residues has been synthesized: Z-Cy2 (QY= 6.8% ± 0.1, ε= 155,000), Z-Cy3 (QY= 11.1% ± 0.4, ε= 124,500), Z-Cy5 (QY= 43.3% ± 0.6, ε= 217,600). In addition, a complete three dye zwitterionic saturation labeling set which incorporates a cysteic acid motif and maleimide functionality reactive towards cysteine residues has also been synthesized: Z-Cy2-Mal (QY= 6.6 % ± 0.1, ε= 104,500), Z-Cy3-Mal (QY= 12.4 % ± 0.5, ε= 127,700), Z-Cy5-Mal (QY= 40.2 % ± 0.4, ε= 217,400).

FLUOROESCENT DYES AND PROTEOMICS

Fluorescent Dyes

Fluorescent molecules have long been targets of interest for organic synthesis. The historical pursuit of these molecules stems from the advantages of utilizing the properties of fluorescence as an analytical probe[1]. Fluorescence is highly sensitive allowing for large dynamic range and increased lower limits of quantitation, in relatively low concentrations[2]. The ability to tune the excitation and emission wavelengths of the fluorophore has sparked a variety of fluorophore moieties to be explored[1]. The attunement of application driven fluorophores has been a fruitful venture producing a variety of dyes, for example: fluorescein, rhodamine, and cyanine[1]. Desirable fluorophore properties include a high quantum yield, pH insensitivity, compatible excitation and emission wavelengths.

Since the synthetic exploration into these types of compounds has been application driven, there are naturally other molecular properties of interest beyond the properties of the fluorophore which must be taken into consideration. Dye properties extending beyond the fluorophore can be tuned via modification to pendent groups attached to a central fluorophore moiety. Such designable characteristics include but are not limited to: molecular charge, charge stability over a broad range of pH's and diverse reactive functionalities for proteomic specific tagging purposes.

Proteomics

Two areas of study where fluorescent dyes have been essential include genomics and proteomics[1]. The post-genomics era has sought to provide insight past the static views provided by studying the genome, mainly by gaining insights into the dynamic nature of proteins inferred by their rapid change in abundance[3]. Due to the reliance of cellular functions to be dictated by proteins, it is prudent to gather a greater understanding of the role played by proteins in all pertinent functions[3]. Electrophoresis techniques have long provided insight into the up or down regulation of proteins. Two dimensional difference gel electrophoresis (2D-DIGE) provides relatively high data throughput without absolute dependence on the mass-spectrometer[4].

Gel electrophoresis is a well-established technique designed to separate proteins in one dimension based upon charge and or size[5]. This technique can be used as preparation for subsequent analytical techniques such as mass spectrometry[4]. A major advancement in the field came in the form of two- dimensional gel electrophoresis (2DE). This advancement allowed for proteins to be separated based upon two orthogonal properties, mass and charge[6]. A limitation of 2DE is the inability to run multiple protein samples, i.e. control and experimental lots, on the same gel. This limitation makes direct abundance comparisons difficult and requires time consuming repeats to attain statistically relevant comparisons[6]. The solution to this problem came about with the development of 2D-DIGE[6]. When applying the 2D-DIGE technique up to three different protein samples, i.e. control, experimental, and an internal standard that combines the two are labeled separately with three different fluorescent dyes which have unique excitation

wavelengths. The labeled protein samples are then mixed and resolved on a single gel. The proteins are detected by acquiring fluorescent images, utilizing the specific excitation wavelength of the different dyes. This allows for direct comparison of protein abundance of the control and experimental samples without time costly repeats. Also the internal standard allows for comparison of multiple gels[6]. Below is Figure 1.1, illustrating the fundamental flow of the 2D-DIGE technique[7]:

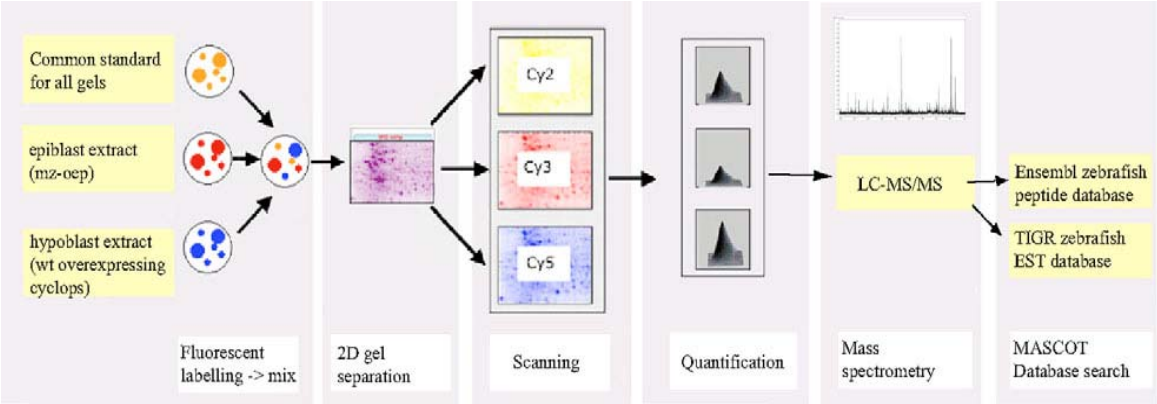

Figure 1.1. General Outline of the 2D-DIGE Technique.

Dyes in Proteomic Applications

The development of the 2D-DIGE technique created a need for fluorescent dyes which possess a reactive motif allowing for facile attachment to proteins. Two such reactive motifs are a succimide ester which is appropriate for attachment to available primary amines such as is present in lysine (Lys) and a maleimide motif which is reactive toward the thiol functionality present in cysteine (Cys)[8]. There are many considerations which must be accounted for when designing dyes for such a sensitive application. This

has led to over a decade of dye development[6]. Numerous fluorophore's have been utilized and the variations of pendent group functionalization have been well explored.

The concerns which arise from the use of the commercially available the CyDyes are issues with changing the proteins untagged characteristics such as aqueous solubility and isoelectric point (pI)[12]. Changes in characteristics of this nature can affect protein separation during electrophoresis and therefore need to be addressed in the design of the applicable dyes as to minimize such problems.

Separation issues arising from change in mass due to labeling is something which cannot be completely avoided. Any dye which is attached to a protein will inherently change the mass of that protein to a certain degree. To minimize the problem of changing protein mass, dyes which have relatively low molecular weight can be employed. Dye sets are also designed in such a way that the unique dyes have similar molecular weights, such that the different proteins to be separated using 2D-DIGE will all be effected proportionally by the inherent change in mass due to protein labeling[3].

Aqueous solubility has been a problem which has plagued the standard cyanine dyes commonly utilized for 2D-DIGE. Structurally these dyes are non-polar, which inhibits aqueous solubility. The structures of these standard dyes can be seen below in Figure 1.2:

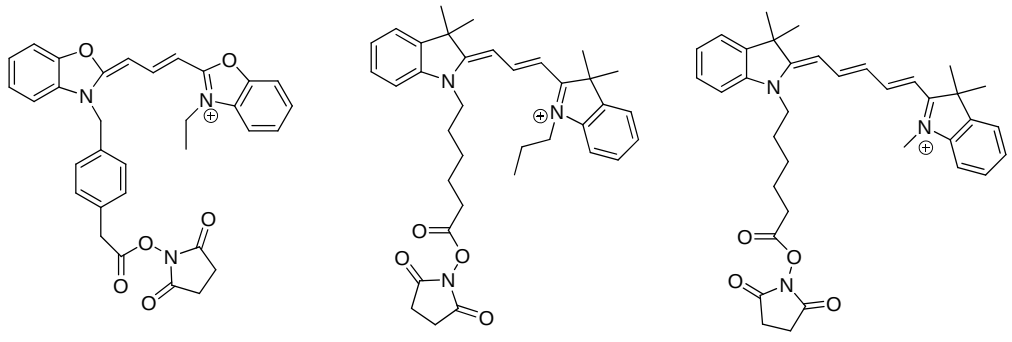

Figure 1.2. GE Healthcare Life Sciences:
Amersham CyDye DIGE Fluors (minimal dyes).

Since these dyes are reactive towards the relatively abundant Lys residue, protein precipitation can occur as a result of over labeling. To overcome this issue which is propagated by the dye's inherent solubility issues, minimal labeling techniques are utilized[9]. In this technique approximately five percent of the Lys residues present in a protein are labeled, providing a dye concentration adequate for detection while not inducing precipitation of the tagged protein samples[9].

One way to overcome protein precipitation due to over labeling is to employ a saturation labeling technique. This technique attaches dyes to Cys residues, which are statistically less abundant than the Lys residue[10]. Since the Cys residue is reactive towards the maleimide motif, protein precipitation by over labeling is avoided by the statistical advantage of having less Cys residues available for labeling. Therefore an excess of dye is used during the protein labeling step, providing 100-200 times greater sensitivity than the minimal labeling technique previously discussed[2]. This technique significantly reduces the amount of protein needed; an advantage when using precious biological samples[2].

Functionalization with a sulfonate moiety on the fluorophore has been a common strategy for increasing the solubility of fluorescent dyes[11]. While the installation of the sulfonate group onto the dye leads to increased aqueous solubility it also causes charge imbalances which can affect a tagged protein's pI. This problem was previously resolved within the Grieco research group through the installation of a sidechain which incorporates a cysteic acid, a titratable amine motif which provide charge balance and allows the labeled protein to have the same charge as when unlabeled over a greater pH range[12].

The dye set consisted of three unique boron-dipyrromethene, BODIPY fluorophores: blue **XV**, green **XVI** and red **XVII**. These dyes are coined "Z-Dyes" corresponding to their zwitterionic structure and can be seen below in Figure 1.3:

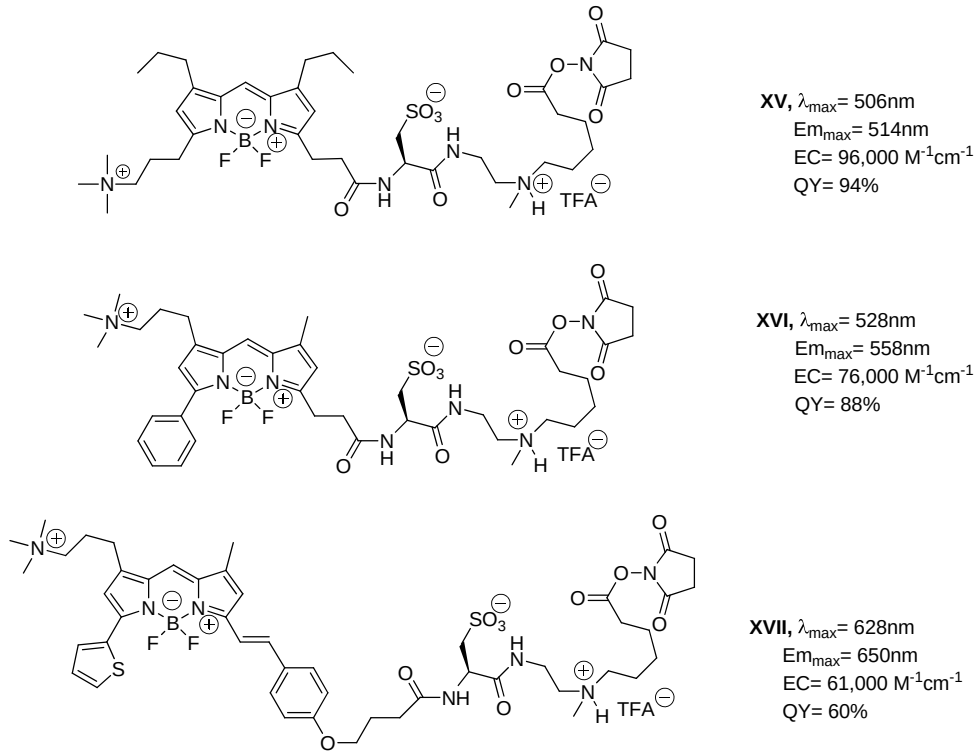

Figure 1.3. BODIPY Z-Dye Set.

Two distinct technical disadvantages inhibited this family of BODIPY dyes. The first issue arouse in respect to the red fluorophore **XVII**, which was susceptible to Michael addition at its vinylic position resulting in a change of the dyes emission profile. The second disadvantage stemmed from the pH sensitivity of the green fluorophore **XVI**, which lost its fluorescent properties at pH's below 3.5 and above 11.With these limitation in mind it was clear that a more robust family of dyes was needed. Thus the aim of this project was to prepare a dye set of three dyes for use in 2D-DIGE, combining the commercially available CyDye fluorophores with the aqueous solubility enhancing and pI matching properties imparted by the cysteic acid, titratable amine sidechain. The synthetically targeted dyes are depicted below in Figure 1.4:

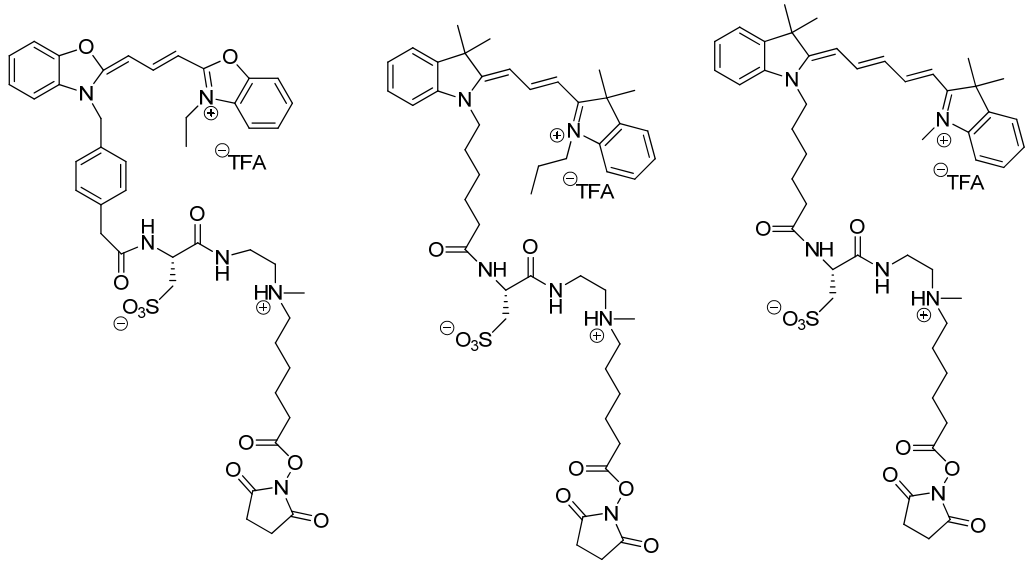

Figure 1.4. Synthetic Target: Z-CyDye Set.

SYNTHESIS OF DYES

Synthesis of Cyanine Fluorophores

There are numerous iterations of the basic cyanine motif, which was disclosed by Waggoner *et al* in 1989.[13] The Amersham group, now, GE have produced the commercially available CyDye DIGE minimal labeling set of dyes consisting of Cy2, Cy3 and Cy5. More recently, a convenient synthesis of these CyDye fluorophores was articulated by Jung and collaborators[14].

The Jung synthesis was utilized to access the cyanine fluorophores of interest, which were then subjected to further functionalization. Cy2 **1** was accessed starting with *N*-alkylation of 2-methylbenzoxazole **I** with ethylbromide to obtain **II**, followed by condensation with *N,N'*-diphenylformamidine to obtain the benzoxazolium salt **III** (Scheme 2.1). It should be noted that **II** is commercially available as the iodide salt and was procured as such for the synthesis outlined herein[15].

With the benzoxazolium salt **III** in hand, attention was turned to the synthesis of **IV**. *N*-Alkylation of **I** with 4-bromomethylphenylacetic acid in 1,2-dichlorobenzene at 110^{o}C produced **IV**. Condensation of compounds **III** and **IV** in ethanol, in the presence of triethylamine yielded the free **V**. Activation of **V** was accomplished by reaction with *N,N'*-disuccinimidyl carbonate in the presence of pyridine yielding the NHS ester **1**.

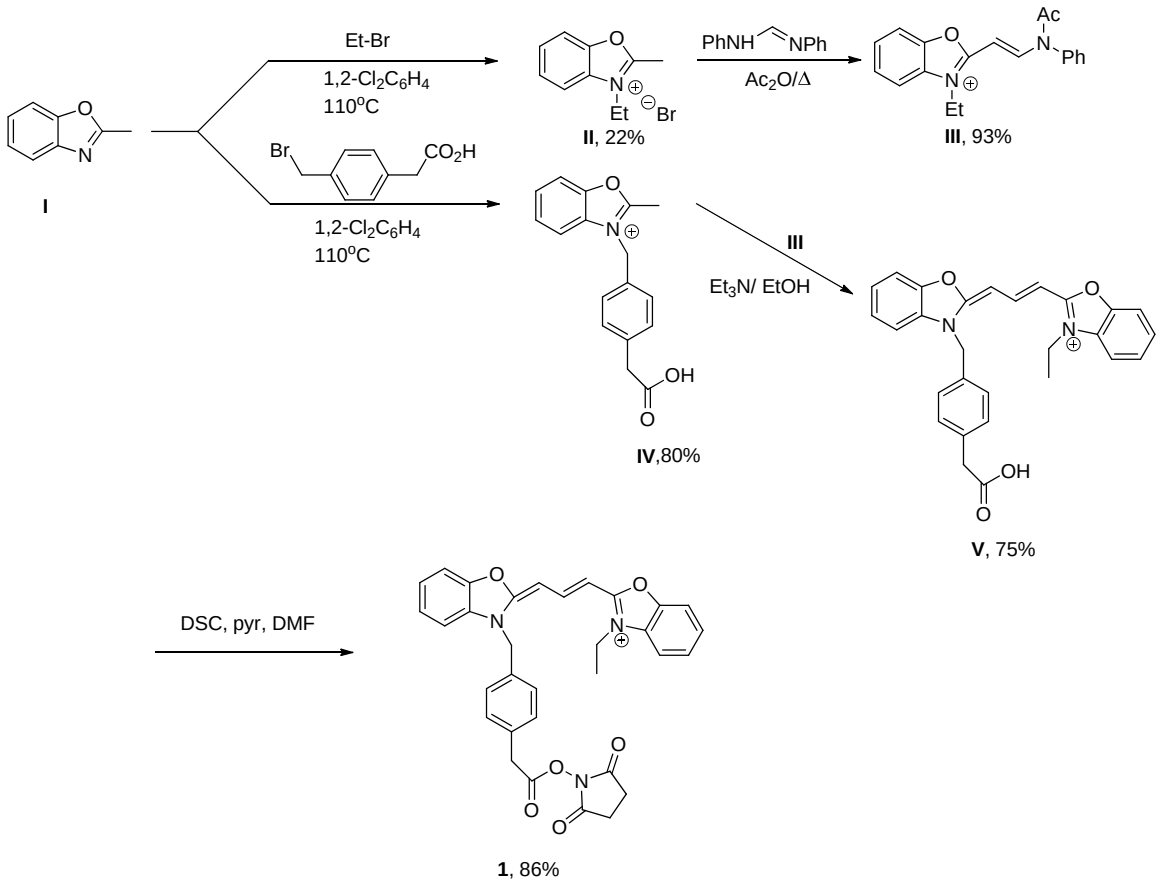

Scheme 2.1. Synthesis of the Succinimide Activated Cy2 Dye.

The synthesis of the Cy3 dye began with the *N*-alkylation of 2,3,3-trimethyl-3*H*-indole **VI** with 1-bromopropane providing the hydrobromide salt **VII** (Scheme 2.2). Subsequent condensation of **VII** with *N,N'*-diphenylformamidine yielded the indolium salt **VIII**. Synthesis of the indolium salt **IX** was accomplished via the *N*-alkylation of **VI** with 6-bromohexanoic acid. Condensation of compounds **VIII** and **IX** in in the presence of triethylamine afforded the free acid **X**. The free acid was activated using the conditions detailed above, which gave rise to the NHS ester **2**.

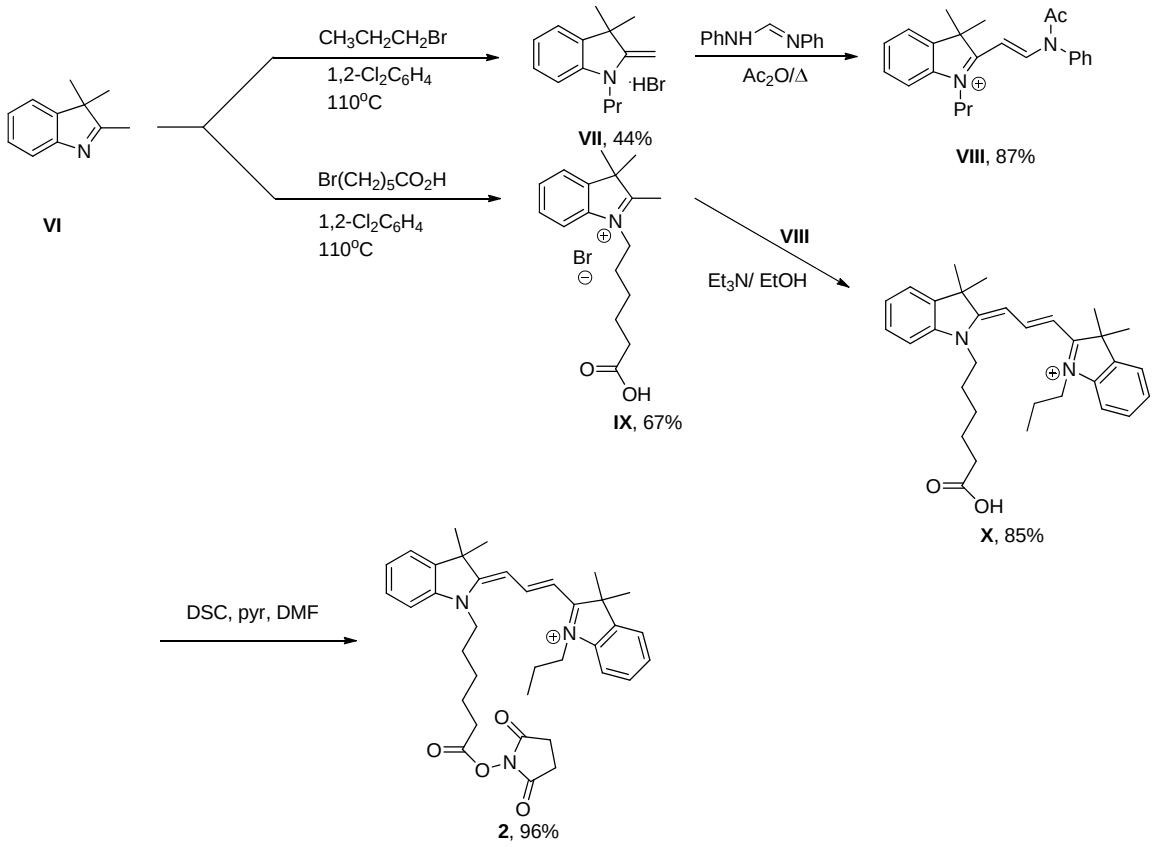

Scheme 2.2. Synthesis of the Succinimide Activated Cy3 Dye.

Synthesis of the Cy5 fluorophore utilized the *N*-alkylated fragment **IX** previously employed in the synthesis of Cy3 **2**. The indolium salt **VIII** was accessed via a two-step protocol. Condensation of 1,1,3,3-tetramethoxypropane with aniline, under acidic conditions generated the aniline anilinium salt **XII**. Subsequent condensation of **XII** with 1,3,3-trimethyl-2-methyleneindoline in neat acidic acid produced the indolium salt **XIII**. Coupling of **XIII** and **IX** in the presence of sodium acetate yielded free acid **XIV.** The acid **XIV** was converted to the NHS ester **3**, using the conditions previously described (Scheme 2.3).

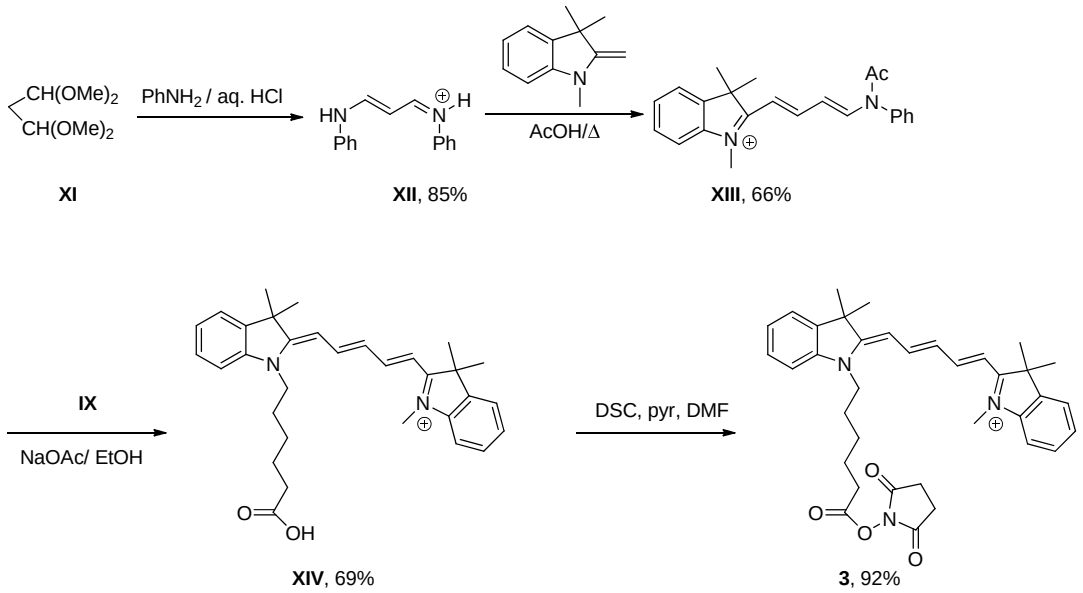

Scheme 2.3. Synthesis of the Succinimide Activated Cy5 Dye.

Synthesis of the Cysteic Acid/Titratable Amine Sidechain

The common functionality across all the Z-CyDyes is the cysteic acid derived sidechain which contains a titratable amine motif **XXVII** (Figure 2.1). The sidechain **XXVII** was previously utilized in the BODIPY family of dyes which were realized through efforts in the Grieco research group.

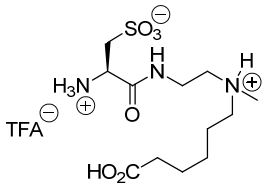

XXVII

Figure 2.1: Cysteic Acid Sidechain with the Titratable Amine Functionality.

The cysteic acid sidechain was produced in nine synthetic steps starting with commercially available *N*-methylcaprolactam **XVIII**[12]. The synthesis commenced with ring opening hydrolysis of **XVIII** which gave rise to the acyclic intermediate **XIX**. The resulting amine was protected as its trifluoroacetamide **XX** (Scheme 2.4). Reaction of intermediate **XX** with *tert*-butanol, in the presence of pyridine and phosphoryl chloride led to the conversion of the carboxylic acid into the corresponding *t*-butyl ester **XXI**. Deprotection of the amine in **XXI** using lithium hydroxide in aqueous methanol provided the free secondary amine **XXII**. Reaction of **XXII** with *N*-Boc-bromoethylamine in the presence of aqueous sodium carbonate afforded **XXIII**, which after global deprotection with trifluoroacetic and triethylsilane produced the bis salt **XXIV**.The primary amine derived from **XXIV** was coupled with commercially available Boc-Cys(Trt)-OSu in aqueous dioxane containing sodium carbonate giving rise to **XXV**. Compound **XXV** was subjected to global deprotection using Et_3SiH/TFA/DCM, which afforded the thiol bis TFA salt **XXVI**. Oxidation of the realized thiol afforded the cysteic acid sidechain **XXVII.**

Synthesis of the Cysteic Acid Sidechain for Maleimide CyDyes

To adapt the cyanine fluorophores for use in saturation labeling, a cysteic acid sidechain lacking a titratable amine and bearing a terminal thiol reactive maleimide was designed. The titratable amine is not required for this type of labeling because there is no loss of a positive charge when coupling with a Cys resiude, as occurs when Lys coupling is employed. The linker between the maleimide motif and the cyanine fluorophore was

previously designed and synthesized in the Grieco group utilizing the cysteine derived specialty reagent, Boc-Cys(Trt)-OSu in three synthetic steps. Coupling of Boc-Cys(Trt)-OSu with 5-aminovaleric acid hydrochloride **XXVIII** produced the fully protected cysteine fragment **XXIX** (Scheme 2.5). Global deprotection of **XXIX** was realized using Et_3SiH/TFA/DCM generating **XXX**, which upon performic acid oxidation gave rise to cysteic acid sidechain **XXXI**[16].

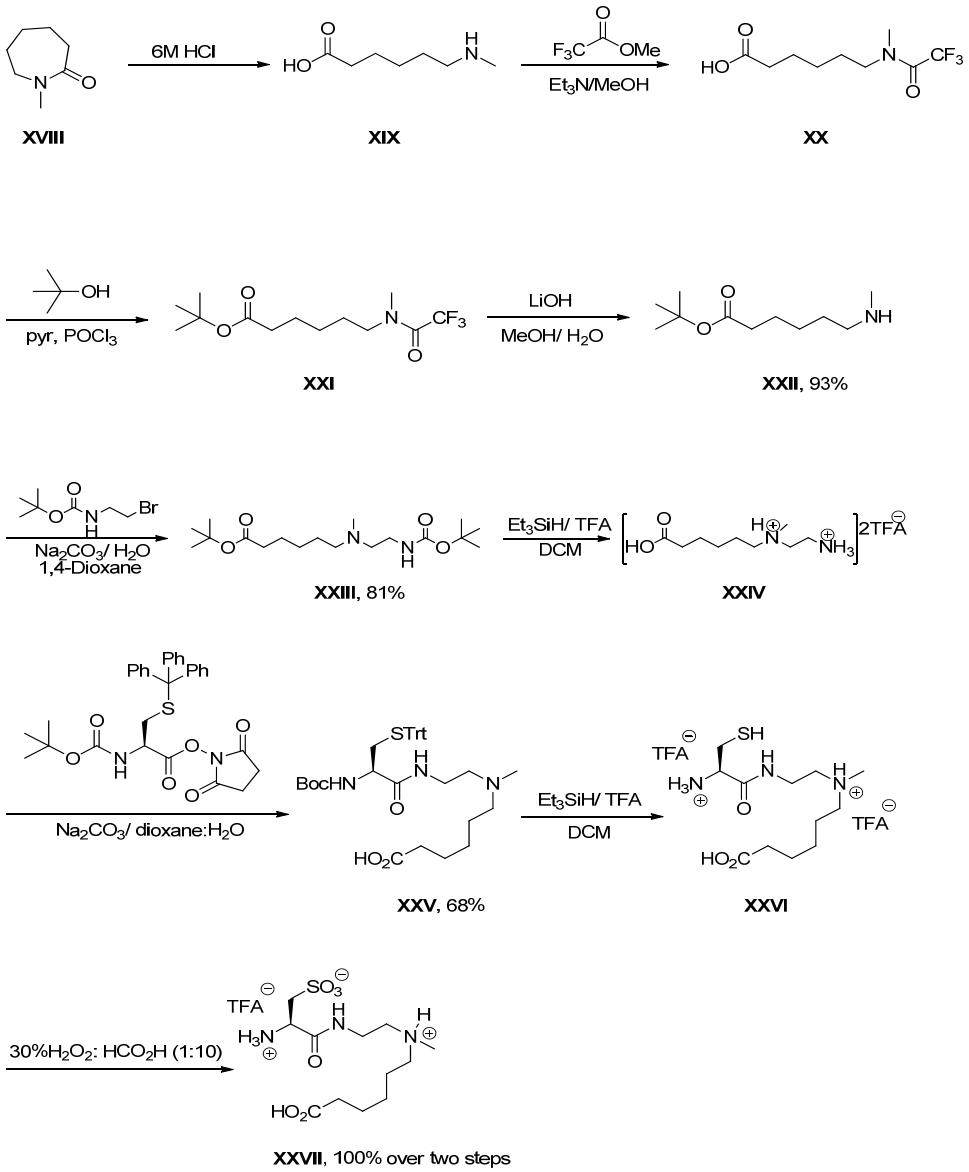

XVIII **XIX** **XX**

XXI **XXII**, 93%

XXIII, 81% **XXIV**

XXV, 68% **XXVI**

XXVII, 100% over two steps

Scheme 2.4. Synthesis of the Cysteic Acid, Titratable Amine Sidechain.

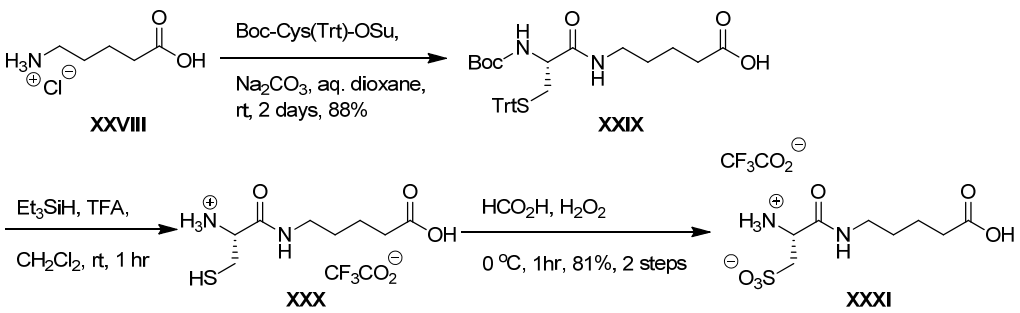

Scheme 2.5. Synthesis of the Cysteic Acid Sidechain.

FUNCTIONALIZATION OF CYNANINE FLUOROPHORES

Z-CyDyes

Having prepared the CyDye set following the protocol set forth by Jung *et al*. The three dyes were all prepared using the same protocol, which is illustrated for Cy2 (Scheme 3.1). The activated NHS ester CyDye fluorophores were subjected to peptide coupling with the titratable amine containing cysteic acid sidechain **XXVII**[12,14]. Coupling of the activated Cy2 fluorophore **1** with **XXVII** (20 equiv. NMM/ DMF) at ambient temperature provided **4** in a 46% yield. Identical couplings were realized for the activated Cy3 fluorophore **2**, resulting in compound **5** in 79% yield and the activated Cy5 fluorophore **3** resulting in compound **6** in 77% yield.

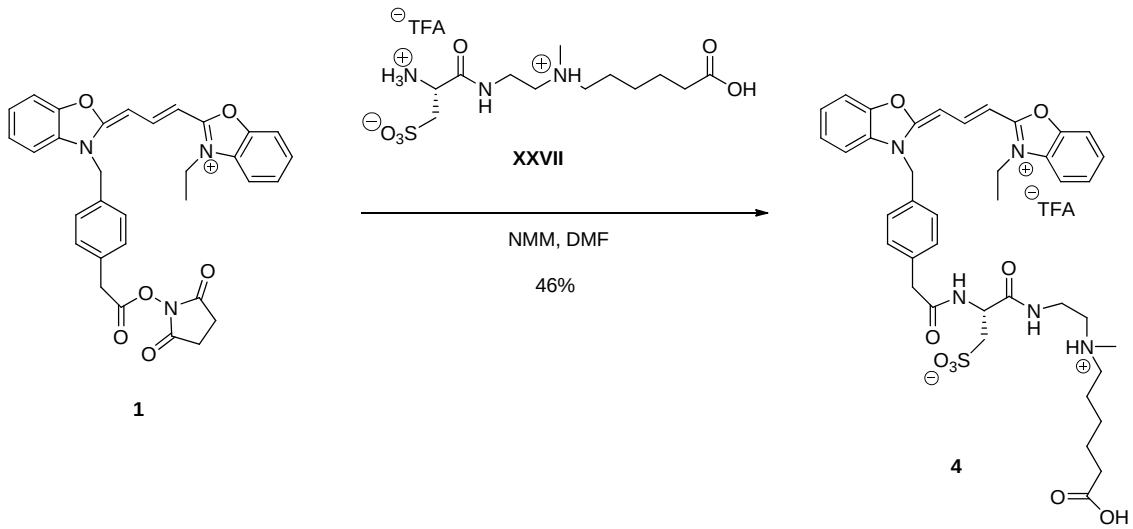

Scheme 3.1. Installation of the Cysteic Acid, Titratable Amine Sidechain.

With the titratable amine sidechain installed on the cyanine dye framework, attention was focused on the activation of the resulting carboxyl functionality. Initally

N,N′-dicyclohexylcarbodiimide (DCC) was utilized for the activation of the Z-CyDye free acid compounds **4-6.** However issues with purification arose due to the presence of the urea resulting from reaction involving DCC. For example activation of free acid **4** employing DCC did give rise to the NHS activated Z-Cy2 **7**, however the yield after purification was only 37% yield, due to the difficulties associated with separating the product **7** from *N,N'*-dicyclohexylurea (Scheme 3.2).

Similar separation issues were encountered during activation of **5** and **6** using DCC and *N*-hydroxysuccimide (NHS). In order to circumvent the separation issues cause by DCC, a water soluble variant of DCC1-ethyl-3-(3-dimethylaminopropyl) carbodiimide (EDC·HCl) was tried and the reactions were monitored via reverse phase HPLC, however no activation of the fluorophores **5** and **6** was detected.

Surprisingly use of *N,N′*-diisopropylcarbodiimide (DIC) proved successful for NHS the activation. For example activation with DIC of the free acid **5** provided compound **8** in 48% yield. Likewise free acid **6** was activated to realize **9** in 76% yield. The best yields were obtained using nine equivelments of DIC in DMF at ambient temperature.

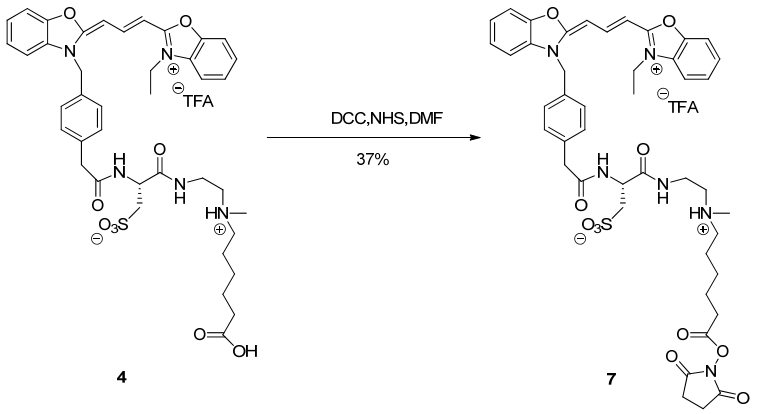

Scheme 3.2. NHS Activation of the Z-CyDye Set.

Z-CyDyes **7-9** (Figure 3.1) were fully characterized by ^{1}H and ^{13}C NMR, HRMS, and IR spectroscopy.

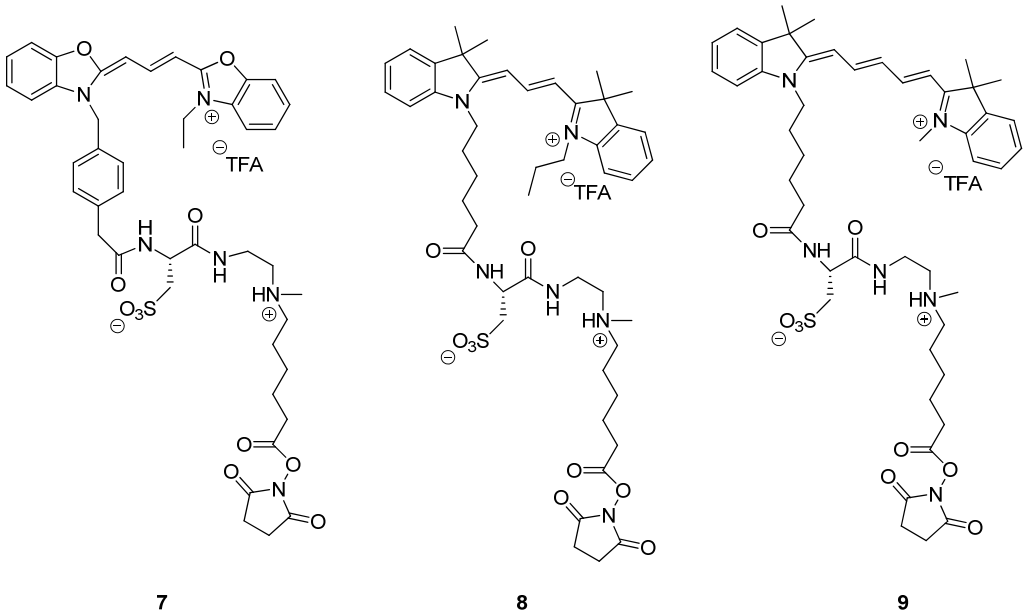

Figure 3.1. Z-CyDye Set.

CyDye-Maleimide Dyes

Once the Z-CyDye NHS ester set was complete, attention was focused on construction of the novel saturation labeling set derived from the same CyDye fluorophores. To accomplish this it was decided to functionalize the cyanine fluorophores with a cystic acid sidechain bearing a terminal maleimide functional group which would be reactive towards the thiol functionality found in cysteine residues.

The zwitterionic CyDye-Maleimide (Z-CyDye-Mal) series began with the activated succimide ester activated cyanine fluorophores (**1-3**) previously described in this thesis. For example the activated Cy2 fluorophore **1** was coupled with the non-titratable cysteic acid derived sidechain **XXXI** (20 equiv. NMM, DMF). The result of which was **10** in 57% yield (Scheme 3.3). The same peptide coupling was realized for the Cy3 acitvated fluorophore **2**, giving compound **11** in 57% yield and the Cy5 activated fluorophore **3** provided **12** in 52% yield. Subsequent NHS activation (11 equiv. DIC, 13 equiv. NHS, DMF) of compound **10** provided succinimidyl ester **13** in 43% yield. Identical activation of compounds **11** and **12** resulted in products **14** in 54% yield and **15** in 69% yield respectively. The activated NHS ester **13** provided an appropriate electrophilic motif for coupling with the terminal amino group derived from *N*-(5-amino-3-oxapentyl) maleimide trifluoroacetate **XXXII**, which had been previously synthesized in the Grieco group following the procedure of Weber *et al*.[16,17] Condensation of compound **13** with **XXXII** (20 equiv. NMM, DMF) afforded Z-Cy2-Mal **16** in 38% yield. Identical condensations were performed for compounds **14** and **15** realizing compounds **17** in a 54% yield and **18** in a 45% yield respectively.

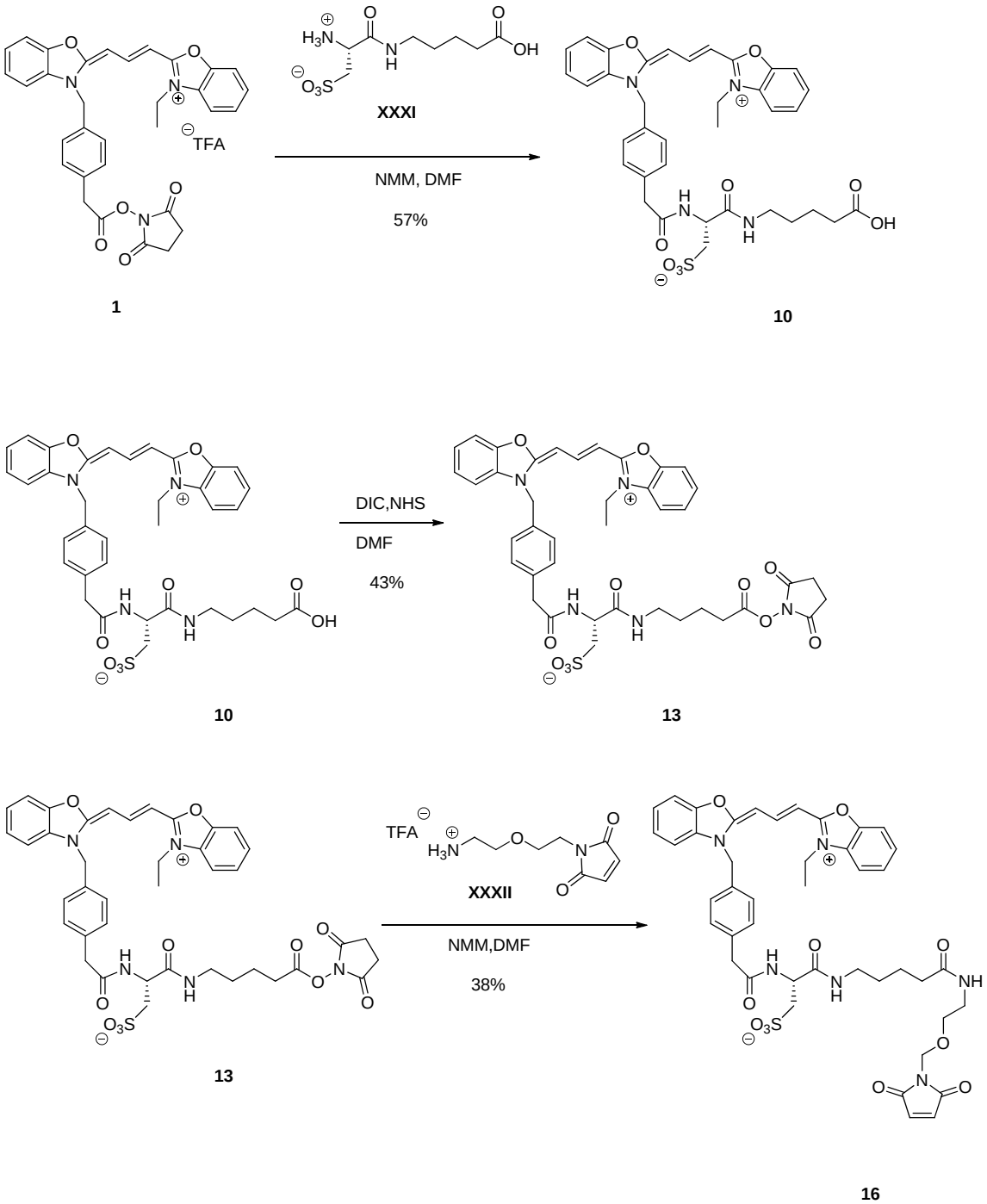

Scheme 3.3. Synthesis of Z-Cy2-Mal.

In summary, the saturation labeling Z-CyDye-Mal dyes (Figure 3.2) were obtained in reasonable yields over a three step synthetic protocol, starting from the

previously realized NHS activated cyanine fluorophores. The Z-CyDye-Mal dyes **16-18** were fully characterized by ^{1}H and ^{13}C NMR, HRMS, and IR spectroscopy.

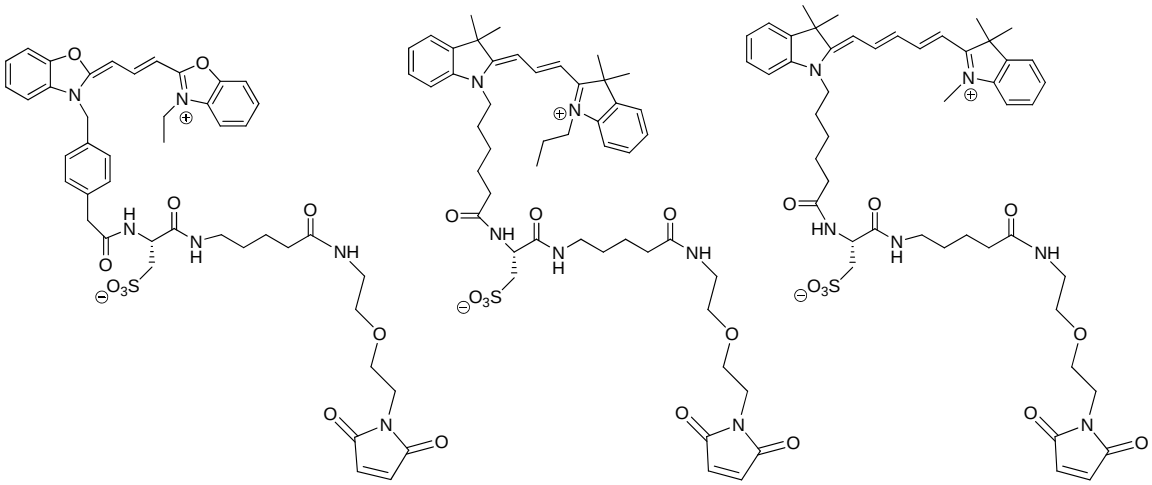

16 **17** **18**

Figure 3.2. Z-CyDye-Mal Set.

OPTICAL CHARACTERIZATION

Optical Characterization of Z-CyDye and Z-CyDye-Mal Sets

After successful structural characterization of the Z-CyDyes **7-9** and Z-CyDye-Mals **17-19** sets were completed, optical characterization of the dyes was undertaken. Absorbance and emission profiles for each dye were determined using both a Varian Cary 6000i UV-VIS NIR Spectrophotometer using a data interval of 0.25 nm, a scan rate of 150 nm/min, a band width of 2 nm and a Varian Cary Eclipse Fluorescence Spectrophotometer, using a scan rate of 120 nm/min and a bandwidth of 5 nm. Anhydrous methanol was used as the spectroscopic solvent, utilizing 1 cm cuvettes for both absorbance and emission readings. Molecular extinction coefficient values were determined by finding the slope of the concentration versus absorbance at λ_{max}. The results from Z-Cy5 are shown below in Figure 4.1.

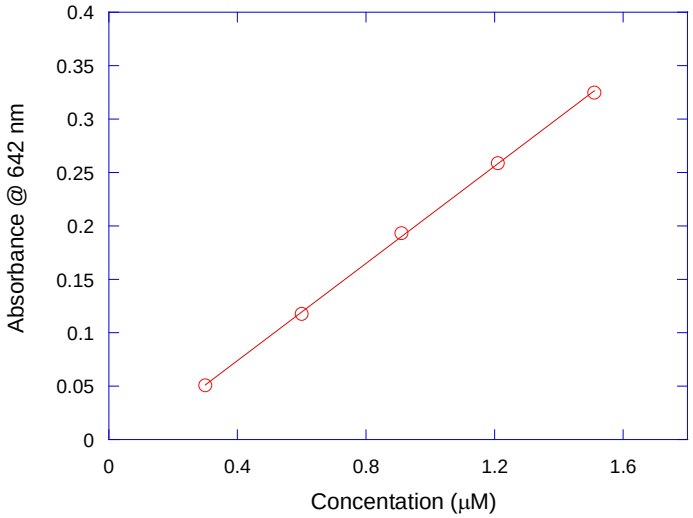

Figure 4.1. Molar Absorptivity: Z-Cy5

Quantum yields were determined in triplicate by comparing novel dyes **7-9** and **16-18** to reference dyes **19-21** with established quantum yields.[18],[19],[20] The reference dyes can be seen in Figure 4.2. It should be noted that the reference dye **21** for the Cy5 based fluorophores was synthesized in house, as it was not found to be commercially available.

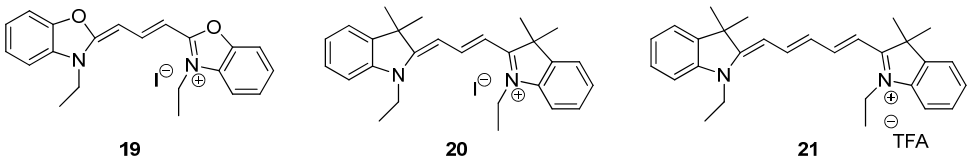

$\lambda_{excit.}$ = 450nm
QY: 5%[22]

$\lambda_{excit.}$ = 500nm
QY: 7%[22]

$\lambda_{excit.}$ = 590nm
QY: 40%[23]

Figure 4.2. Quantum Yield Standard Dyes

Dilution series' were made with a maximum absorbance of 0.1 at the prescribed wavelength (based on the reference dye) to ensure minimization of the inner filter effect and non-radiative emission caused by aggregation. Emission spectra for the novel dyes **7-9** and **17-19** along with the CyDye DIGE Fluors were collected using the same excitation wavelength and parameters used to find the quantum yield of the standard dyes. Figure 4.3 shows the absorbance profile for Z-Cy5 at five different concentrations. The absorbance values were measured at 590 nm for quantum yield determination.

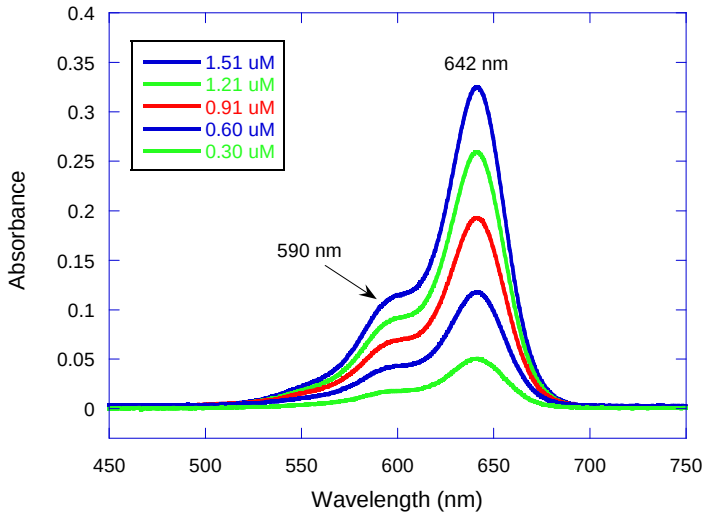

Figure 4.3. Absorbance Profile of Z-Cy5

Corresponding emission data was collected for the dyes with the same concentration series as were used for the absorbance data. Fluorescence profiles were aquired with an excitation wavelength that matched the wavelength at which the absorbance readings were determined. Below in Figure 4.4 is the emission profile for Z-Cy5.

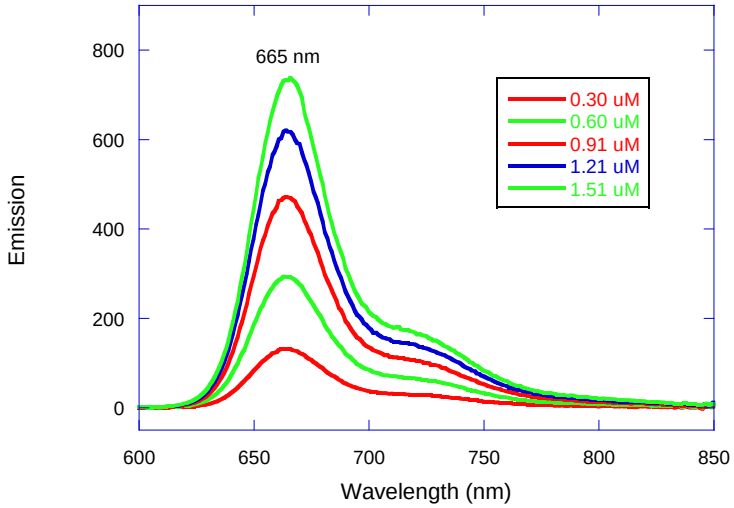

Figure 4.4: Emission Profile of Z-Cy5

By plotting the absorbance at the excitation wavelength against the corresponding intergrated flourescence, a linear slope (m) was fitted. Below in Figure 4.5 is a plot showing such a slope for the Z-Cy5 dye.

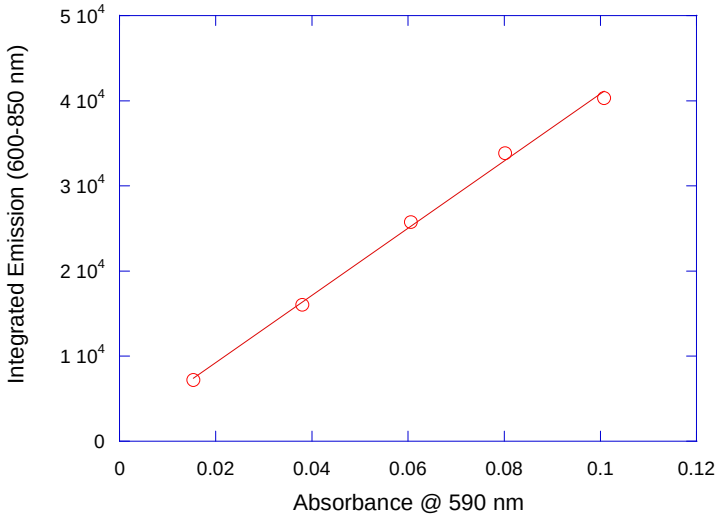

Figure 4.5: Intergrated Emission vs. Absorbance of Z-Cy5

Once the slopes for the standard dyes and the novel dyes were ascertained, the values were inputted into the equation seen in Figure 4.6:

$$Q=Q_{std}(m/m_{std})(n^2/n_{std}^2)$$

Figure 4.6. Quantum Yield Equation

where Q is the quantum yield of the experimental dye, Q_{std} is the established quantum yield of the appropriate reference dye; m and m_{std} are the slopes of the experimental and reference dyes respectively; n and n_{std} are the refractive indexes of the solvents used. Since the same solvent was used for both the novel dyes and the corresponding reference

dyes, this term goes to unity. The results of the triplicate quantum yield calculations and the molar extinction coeffeinets for the Z-Cydyes and CyDye DIGE Fluors are summarized below in Table 4.1:

Dye	λ_{max} (nm)	Em_{max} (nm)	QY (%)	ε ($M^{-1}cm^{-1}$)
Z-Cy2 **7**	485	500	6.8±0.1	155,000
Cy2 DIGE Fluor	485	501	6.3±0.2	150,300
Z-Cy3 **8**	518	564	11.1 ±0.4	124,500
Cy3 DIGE Fluor	518	564	9.9 ± 0.1	137,600
Z-Cy5 **9**	642	665	43.3 ± 0.6	216,200
Cy5 DIGE Fluor	642	665	37.3 ± 0.3	214,400

Table 4.1. Optical Characterization Summery: Z-CyDyes and CyDye DIGE Fluors

When compared to the established quantum yield values for the CyDye DIGE Fluors the Z-CyDyes exhibit greater values. This may be due to a decrease in fluorophore aggregation caused by the steric and electronic repulsion between the cysteic sidechains, despite the usage of dilute solutions as previously discussed.

Using the same methods described above, the quantum yield and molar extinction coeffient values for the Z-CyDye-Mals were determined (Table 4.2).

Dye	λ_{max} (nm)	Em_{max} (nm)	QY (%)	ε ($M^{-1}cm^{-1}$)
Z-Cy2-Mal	485	500	6.6±0.1	104,500
Z-Cy3-Mal	518	564	12.4 ± 0.5	127,700
Z-Cy5-Mal	642	665	40.2 ± 0.4	217,400

Table 4.2. Optical Characterization Summery: Z-CyDye-Mal dyes

QUANTIFICATION OF 2D-DIGE LABELING COMPARISON

Z-CyDyes and CyDye DIGE Fluors

The Z-CyDyes were tested alongside the CyDye DIGE fluors in triplicate to test their differences in sensitivity for use in 2D-DIGE. Soluble protein samples (50 μg) from the archea thermophillic organism *Sulfolobus solfataricus* were labeled with fluorescent dye (400 pmol/50 μg protein). Standard CyDye, 2D-DIGE protocols were used for all of the labeling reactions and gel experiments. Quantification experiments were completed for Z-Cy3 and Z-Cy5 versus their corresponding CyDye DIGE fluors. The Cy2 DIGE fluor was used as an internal standard for the quantification experiments, such that the different gels could be compared in a meaningful way. Out of approximately 500 spots identified, the spot volumes for 281 spots were measured. These spots were chosen for their well-defined boundaries and ranged in intensity from strong spots to faint spots. Of the 281 spots measured, 223 spots were measured to be more intense when labeled with Z-Cy3 in comparision to the Cy3 DIGE fluor. Of the remaining spots, 54 were measured to be more intense with the Cy3 DIGE fluor and 4 spots were measured at the same intensity with both labeling dyes. Comparison of Z-Cy5 to the Cy5 DIGE fluor gave similar results, with 281 measured spots. Of the measured spots 220 spots were more intense when labeled with Z-Cy5, 53 spots were more intense when labeled with the Cy5 DIGE fluor and 8 spots were measured at the same intensity. Figure 5.1 provides an example of the evaluation of a single spot, illustrating the differences in spot intensity measure for Z-Cy3, Z-Cy5 and the DIGE fluors Cy3, Cy5. The normalized volume used

in the comparison is a logarithmic ratio of a given dye over the internal standard dye, Cy2.

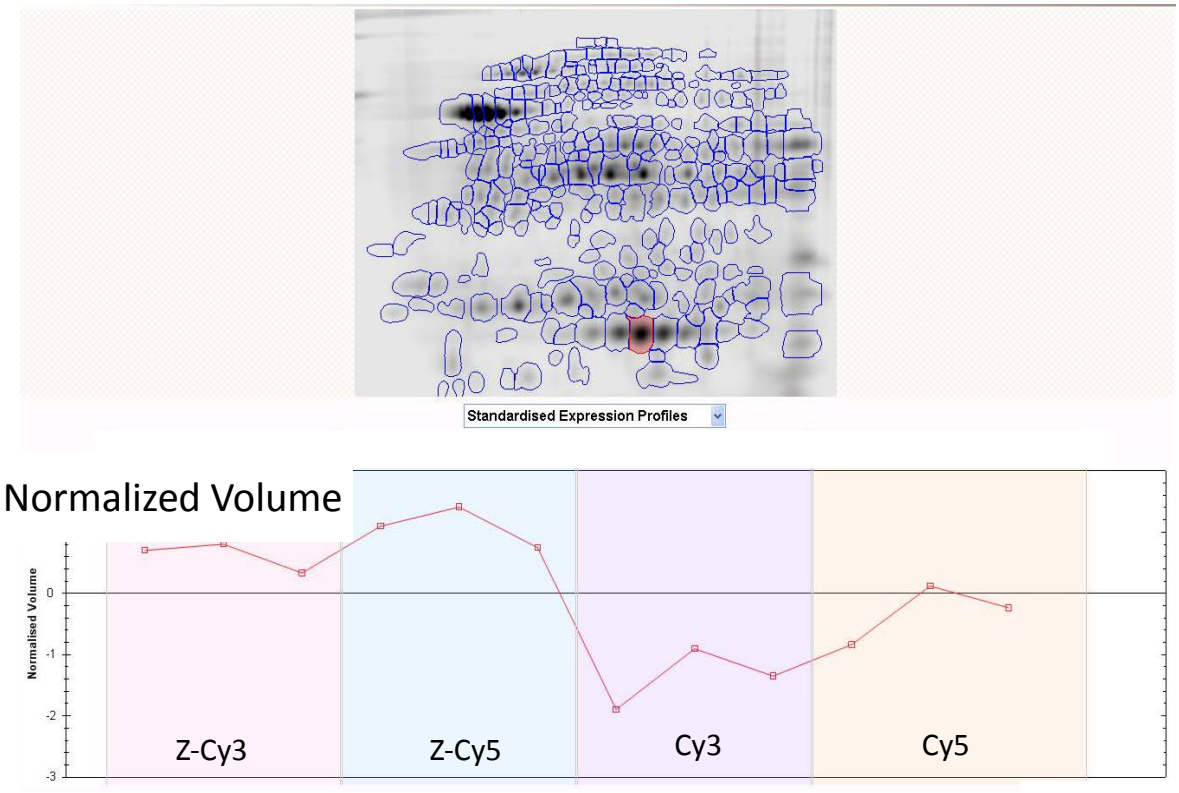

Figure 5.1. Comparison of Spot 191

Figure 5.2 plots the difference in spot volume (%) of Z-Cy5 vs. the Cy5 DIGE fluor and Z-Cy3 vs. the Cy3 DIGE fluor. It is important to note that the spot volume differences are much greater when Z-Cydyes are more intense (up to 70% increase) in comparison to the spot volume differences when Cydyes are more intense (up to 20% increase). From these results it is clear that the Z-CyDyes exhibit improved sensitivity over the CyDye DIGE fluors.

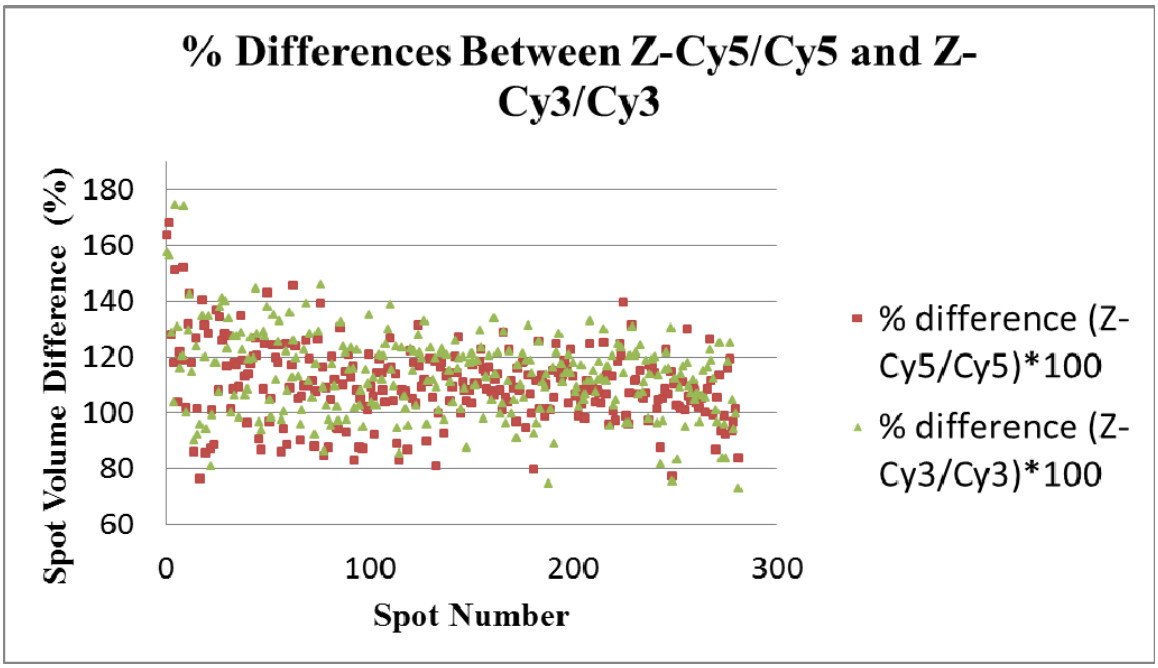

Figure 5.2. Spot Volume Percent Difference Comparison

REFERENCES CITED

[1] Waggoner, A. *Current Opinion in Chemical Biology,* **2006**, 10, 62-66

[2] Kondo, T.; Hirohashi, S. *Nature Protocols*, **2006**, 6, 2940-2956.

[3] Unlu, M.; Minden, J. *The Protein Protocols Handbook*, **2002**, 185-196

[4] Chevalier, F. *Materials*, **2010**, 3, 4784-4792

[5] O'Farrell, P.H.; *J Biol Chem,* **1975**, 250, 4007-4021.

[6] Unlu, M; Morgan, M.E.; Minden, J. S. *Electrophoresis*, **1997**, 18, 2071-2077.

[7] Link, V.; Carvalho, L.; Castanon, I.; Stockinger, P.; Shevchenko, A.; Heisenberg, C. P. *J Cell Sci,* **2006**, 119, 2073-2083

[8] Righetti, P. G.; Castagna, A.; Antonucci, F.; Piubelli, C.; Ceccconi, D.; Campostrini, N.; Antonioli, P.; Astner, H.; Hamdan, M. *Journal of Chromatography* A, **2004**, 1051, 3-17

[9] Tonge, R.; Shaw, J.; Middleton, B.; Rowlinson, R.; Rayner, S.; Young, J.; Pognan, F.; Hawkins, E.; Currie, I.; Davison, M. *Proteomics,***2001**, 1, 377-396

[10] Cornish-Bowden, A. Biochem J. **1983**, 213, 271-274

[11] Mujumdar, S.R.; Mujumdar, R.B.; Grant, C.M.; Waggoner, A.S. *Bioconjugate Chem*. **1996**, 7, 356-362

[12] Dratz, E.; Grieco, P. U.S. Patent 7,833,799

[13] Mujumdar, R. B.; Ernst, L. A.; Mujumdar, S. R.; Waggoner, A. S. *Cytometry*, **1989**, 10, 11-19

[14] Jung, M. E.; Kim, W. *Bioorganic & Medicinal Chemistry*, **2006**, 14, 92-97

[15] Purchased From Sigma Aldrich, Catalog #376981

[16] Spicka, K. PhD. Dissertation, Montana State University, **2008**

[17] Weber, R.W.; Boutin, R.H.; Nedelman, M.A.; Lister-James, J.; Dean, R.T. *Bioconjugate Chemistry*, **1990**, *1*, 431-437.

[18] Waggoner, A.; DeBiasio, R.; Conrad, P.; Bright, G. R.; Ernst, L.; Ryan, K.; Nederlof, M.; Taylor, D. *Methods in Cell Biology,* **1989**, 30, 449-478.

[19] Ernst, L. A.; Gupta, R. K.; Mujumdar, R.B.; Waggoner, A.S. *Cytometry*, **1989**, 10:3, 10.

[20] Sims, P. J.; Waggoner, A.S.; Wang, C.H.; Hoffman, J. F. Biochem, **1974**, 13, 3315-3330.

APPENDICES

APPENDIX A

EXPERIMENTAL

General Procedure

Nuclear magnetic resonance, both proton (^{1}H NMR) and carbon (^{13}C NMR) were recorded using either a 300 MHz Bruker Avance DPX 300 spectrometer or a 500 MHz Bruker Avance DRX 500 spectrometer and all reports are given in parts per million (δ). ^{1}H NMR spectra were determined in a deuterated solvent, and were referenced against the residual solvent signal: methanol-d_4 (CD_3OD) δ 3.31. ^{13}C NMR spectra were determined in deuterated solvents, and were referenced against the residual solvent signal: dimethyl sulfoxide-d6 (DMSO-d6) δ 39.51 and methanol-d_4 (CD_3OD) δ 49.15. FTIR spectra was acquired on a JASCO FT/IR 4100; samples were dissolved in acetonitrile, placed onto a sodium chloride salt plate and the solvent was evaporated leaving a thin film of sample. Reactions were monitored using reverse phase HPLC utilizing a Shimadzu CBM-2A Prominence Communications Bus Module, Shimadzu SPD-M20A Prominence Diode Array Detector, LC-20AB Prominence Liquid Chromatograph and a Phenomenex Synergi 4µ Polar RP 80Å 250 X 10.00 mm 4 micron column. The mobile phase was always a gradient of HPLC grade H_2O: 95% CH_3CN, 5% H_2O containing 0.1% HPLC grade TFA as ion pairing agent. Reverse phase HPLC purification was carried out using a Waters 600 Pump, a Waters 600 Controller and a Waters 2487 Dual λ Absorbance Detector utilizing a preparative reverse phase Phenomenex Synergi 4µ Polar RP 80Å AXIF 250 mm x 21.20 mm 4 micron column. The mobile phase was always a gradient of HPLC grade H_2O: 95% CH_3CN, 5% H_2O containing 0.1% HPLC grade TFA as ion pairing agent. High resolution mass spectrometry analyses were performed by the University of Notre Dame Mass

Spectrometry Laboratory. Unless noted otherwise all reactions were run under argon using anhydrous solvents. All anhydrous solvents were obtained from SIGMA-ALDRICH in Sure/Seal™ bottles. All other reagents were obtained from SIGMA-ALDRICH and used as received.

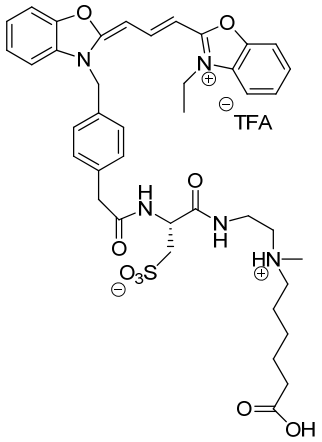

(2R)-3-((2-((5-carboxypentyl)(methyl)ammonio)ethyl)amino)-2-(2-(4-((2-((1E,3Z)-3-(3-ethylbenzo[d]oxazol-2(3H)-ylidene)prop-1-en-1-yl)benzo[d]oxazol-3-ium-3-yl)methyl)phenyl)acetamido)-3-oxopropane-1-sulfonate 2,2,2-trifluoroacetate (4).

2-[3-[3-[[4-[2-[(2,5-Dioxo-1-pyrrolidinyl)oxy]-2-oxoethyl]phenyl]methyl]-2(3H)-benzo-xazolylidene]-1-propenyl]-3-ethyl-benzoxazolium salt **1** (46.9 mg, 0.071 mmol, 1.0 eq) was stirred in dimethylformamide (5.0mL) with 6-(*N*-methyl-*N*-(2-(2-amino-3-sulfatoproionamido)ethyl)amino)hexanoic acid trifluoroacetate **XXVII** (160.1 mg, 0.35 mmol, 5.0 eq) under an inert atmosphere at ambient temperature. To the stirring solution was added 4-methylmorpholine (0.15 mL, 1.4 mmol, 20.0 eq) in a dropwise fashion. The reaction mixture was stirred for 24h, after which the solvent was removed under lyophilization yielding crude product as a deep yellow oil. Purification which was

preformed via reverse phase HPLC (30 to 70% B, 20mL/min, 30min, 450nm, R_t = 15-18min) provided 29.0 mg (46% yield) of the TFA salt **4** as a deep yellow powder: FTIR: 1509, 1565, 1681, 2851, 2922, 3357 cm^{-1}; ^1H NMR (300MHz, CD_3OD): δ 1.25-1.39 (m, 2H), 1.46 (t, *J*= 7.5 Hz, 3H), 1.59-1.82 (m, 2H), 2.30 (t, 2H, *J*= 7.2 Hz), 2.85 (s, 3H), 3.09-3.25 (m, 4H), 3.45-3.59 (m, 6H), 4.25 (q, *J*= 7.5 Hz, 2H), 4.62 (dd, *J*= 7.5, 3.9 Hz, 1H), 5.42 (s, 2H), 6.01 (d, *J*= 13.2 Hz, 1H), 6.04 (d, *J*= 13.5 Hz, 1H), 7.32-7.63 (m, 12H), 8.60 (dd, *J*= 13.5, 13.2 Hz, 1H); ^{13}C NMR (75 MHz, CD_3OD): δ 13.37, 24.76, 25.54, 27.15, 34.66, 35.43, 40.59, 43.28, 52.30, 57.31, 57.35, 57.68, 86.01, 87.07, 112.01, 112.04, 112.13, 112.25, 112.39,112.43, 126.51, 126.58, 126.83, 127.41, 127.53, 128.76, 131.42, 132.37, 132.90, 132.99, 134.02, 137.15, 139.86, 148.53, 148.68, 149.37, 163.82, 164.26, 173.57; HRMS (ESI): Exact mass calcd for $C_{40}H_{48}N_5O_9S$ $[M]^+$ 774.3167, found 774.3168.

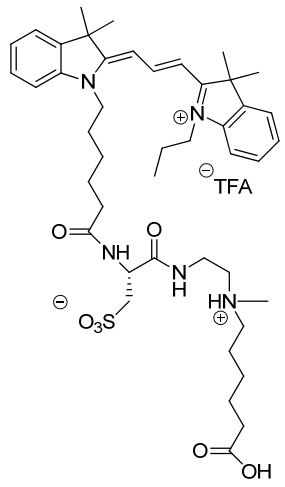

(2R)-3-((2-((5-carboxypentyl)(methyl)ammonio)ethyl)amino)-2-(6-(2-((E)-3-((E)-3,3-dimethyl-1-propylindolin-2-ylidene)prop-1-en-1-yl)-3,3-dimethyl-3H-indol-1-ium-1-yl)hexanamido)-3-oxopropane-1-sulfonate 2,2,2-trifluoroacetate (5).

2-[3-(1,3-Dihydro-3,3-dimethyl-1-propyl-2H-indol-2-ylidene)-1-propenyl]-1-[6-[(2,5-di-oxo-1-pyrro-lidinyl)oxy]-6-oxohexyl]-3,3-dimethyl-3H-indolium salt **2** (15.5 mg, 0.022 mmol, 1.0 eq) was stirred in dimethylformamide (1.6 mL) with 6-(*N*-methyl-*N*-(2-(2-amino-3-sulfatoproionamido)ethyl)amino)hexanoic acid trifluoroacetate **XXVII** (50.33 mg, 0.11 mmol, 5.0 eq) under an inert atmosphere at ambient temperature. To the stirring solution was added 4-methylmorpholine (0.048 mL, 0.44 mmol, 20.0 eq) in a dropwise fashion. The reaction mixture was stirred for 20h, after which the solvent was removed under lyophilization yielding crude product as a deep red oil. Purification which was preformed via reverse phase HPLC (40 to 80% B, 20mL/min, 30min, 530nm, R_t= 12-16min) provided 15.9 mg (79% yield) of the TFA salt **5** as a deep red powder: FTIR: 1478, 1558, 1681, 2938, 3624 cm^{-1} ; ^{1}H NMR (300MHz, CD3OD): δ 1.08 (t, 3H, J=7.3 Hz), 1.28-1.92 (m, 26H), 2.29-2.34 (m, 4H), 2.87 (s, 3H), 2.98-3.24 (m, 4H), 3.44-3.72 (m, 4H), 4.10-4.20 (m, 4H), 4.65-4.69 (m, 1H), 6.49 (d, *J*= 13.2 Hz, 1H), 6.52 (d, *J*= 13.2 Hz, 1H), 7.28-7.56 (m, 8H), 8.40-8.47 (m, 1H) (NH), 8.56 (t, *J*=13.2 Hz, 1H); ^{13}CNMR(75MHz,CD3OD):δ 11.64, 22.07, 24.79, 25.55, 26.30, 27.16, 27.31, 28.33, 28.48, 34.66, 35.37, 35.45, 36.67, 40.86, 40.94, 45.23, 46.79, 50.78, 50.83, 52.02, 52.06, 53.16, 53.26, 57.28, 57.35, 57.68, 103.74, 104.00, 112.66, 112.71, 123.67, 126.91, 130.14, 130.21, 142.33, 142.39, 143.54, 143.64, 152.35, 173.70, 175.61, 175.64, 176.09, 176.36,177.30,177.34; HRMS (ESI): Exact mass calcd for $C_{44}H_{64}N_5O_7S$ $[M]^+$ 806.4521, found 806.4538.

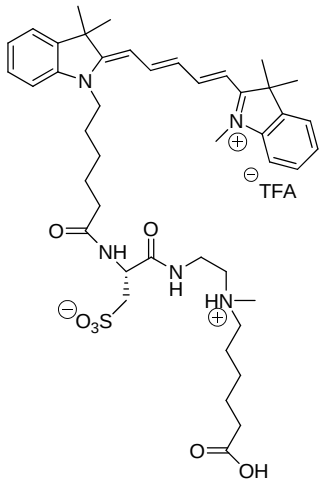

(2R)-3-((2-((5-carboxypentyl)(methyl)ammonio)ethyl)amino)-2-(6-(3,3-dimethyl-2-((1E,3E)-5-((E)-1,3,3-trimethylindolin-2-ylidene)penta-1,3-dien-1-yl)-3H-indol-1-ium-1-yl)hexanamido)-3-oxopropane-1-sulfonate 2,2,2-trifluoroacetate (6).

2-[5-(1,3-Dihydro-1,3,3-trimethyl-2H-indol-2-ylidene)-1,3-pentadienyl]-1-[6-[(2,5-dioxo-1-pyrrolidi-nyl)oxy]-6-oxohexyl]-3,3-dimethyl-3H-indolium salt **3** (22.8 mg, 0.032 mmol, 1.0 eq) was stirred in dimethylformamide (2.2 mL) with 6-(*N*-methyl-*N*-(2-(2-amino-3-sulfatoproionamido)ethyl)amino)hexanoic acid trifluoroacetate **XXVII** (74.4 mg, 0.16 mmol, 5.0 eq) under an inert atmosphere at ambient temperature. To the stirring solution was added 4-methylmorpholine (0.07 mL, 0.64 mmol, 20.0 eq) in a dropwise fashion. The reaction mixture was stirred for 25h, after which the solvent was removed under lyophilization yielding the crude product as a deep blue oil. Purification which was preformed via reverse phase HPLC (60 to 90% B, 20mL/min, 30min, 600nm, R_t= 12-15min) afforded 22.5 mg (77% yield) of the TFA salt **6** as a deep blue powder: FTIR: 1455, 1482, 1496, 1540, 1653, 1682, 2865, 2963, 3545 cm^{-1}; ^1H NMR (300MHz, CD_3OD): δ 1.3-1.69 (m, 6H), 1.73 (s,12), 1.78-1.88 (m, 4H), 2.26-2.36 (m, 4H), 2.88 (s,

3H), 3.00-3.26 (m, 4H), 3.44-3.60 (m, 2H), 3.64 (s, 3H), 3.69- 3.87 (m, 2H), 4.10 (t, *J*=7.2 Hz, 2H), 4.65-4.69 (m, 1H), 6.34 (d, *J*= 13.8, 1H), 6.36 (d, *J*= 13.8, 1H), 6.68 (t, *J*= 12.3, 1H), 7.24-7.51 (m, 8H), 8.25 (dd, *J*= 13.8, 12.3 Hz, 2H), 8.43-8.46 (m, 1H) (NH); ^{13}C NMR (75MHz, CD_3OD): δ 24.78, 24.82, 25.56, 26.25, 27.19, 27.96, 28.11, 28.22, 31.77, 34.66, 35.35, 35.45, 36.44, 40.90, 44.94, 50.66, 52.09, 53.26, 53.33, 57.28, 57.35, 57.63, 57.74, 104.46, 104.77, 112.01, 112.19, 123.42, 123.56, 126.35, 126.41, 126.84, 129.87, 129.95, 142.72, 142.79, 143.71, 144.43, 155.65, 155.77, 173.74, 174.75, 175.61, 175.65; HRMS (ESI): Exact mass calcd for $C_{44}H_{62}N_5O_7S$ $[M]^+$ 804.4364, found 804.4352.

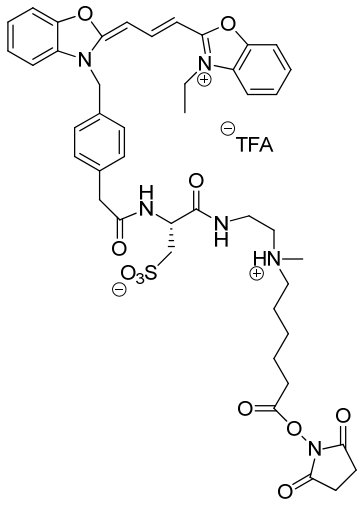

(2R)-3-((2-((6-((2,5-dioxopyrrolidin-1-yl)oxy)-6-oxohexyl)(methyl)ammonio)ethyl)amino)-2-(2-(4-((2-((1E,3Z)-3-(3-ethylbenzo[d]oxazol-2(3H)-ylidene)prop-1-en-1-yl)benzo[d]oxazol-3-ium-3-yl)methyl)phenyl)acetamido)-3-oxopropane-1-sulfonate 2,2,2-trifluoroacetate (7).

Compound **4** (9.7 mg, 0.011 mmol, 1.0 eq) was stirred in dimethylformamide (0.031 mL) with *N*-hydroxysuccimide (6.3 mg, 0.055 mmol, 5.0 eq) under an inert

atmosphere at ambient temperature. To the stirring solution was added *N,N'*-dicyclohexylcarbodiimide (6.8 mg, 0.032 mmol, 3.0 eq) in a dropwise fashion. The reaction mixture was stirred for 25h, after which the solvent was removed under lyophilization yielding crude product as a deep yellow oil. Purification which preformed via reverse phase HPLC (30 to 70% B, 20mL/min, 30min, 450nm, R_t= 19-21min) provided 4.0 mg (37% yield) of the TFA salt **7** as a deep yellow powder: FTIR: 1461, 1507, 1560, 16712, 1741, 2858, 2938, 3063, 3331 cm^{-1}; ^1H NMR (300MHz, CD_3OD): δ 1.23-1.41 (m, 2H), 1.45 (t, *J*= 7.5 Hz, 3H), 1.69-1.85 (m, 4H), 2.66 (t, *J*= 7.2 Hz, 2H), 2.81 (s, 4H), 2.85 (s, 3H), 3.10-3.25 (m, 4H), 3.46-3.66 (m, 6H), 4.25 (q, *J*= 7.5 Hz, 2H), 4.58-4.66 (m, 1H), 5.41 (s, 2H), 6.00 (d, *J*= 13.2 Hz, 1H), 6.05 (d, *J*= 13.2 Hz, 1H) 7.34-7.66 (m, 12H), 8.29-8.44 (m, 1H) (NH), 8.59 (t, *J*=13.2 Hz, 1H); ^{13}C NMR (75 MHz, CD_3OD): δ 13.39, 24.50, 25.16, 25.19, 26.22, 26.65, 31.39, 34.92, 35.36, 35.42, 40.60, 40.90, 40.97, 43.26, 43.31, 52.32, 53.00, 53.15, 57.37, 57.55, 86.00, 87.07, 112.01, 112.13, 112.25, 112.38, 126.57, 126.83, 127.41, 127.53, 128.78, 131.42, 131.45, 132.36, 132.99, 134.02, 137.12, 137.18, 148.52, 148.67, 149.25, 149.33, 163.80, 164.24, 170.31, 172.02, 173.49, 173.56; HRMS (ESI): Exact mass calcd for $C_{44}H_{51}N_6O_{11}S$ $[M]^+$ 871.3331, found 871.3340.

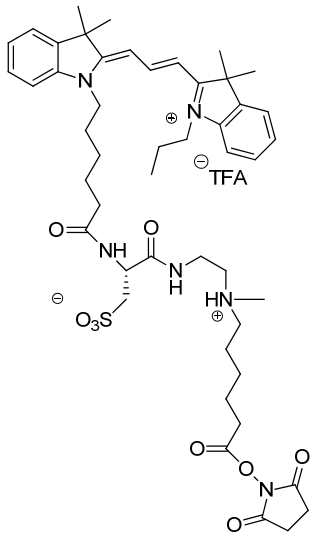

(2R)-2-(6-(2-((E)-3-((E)-3,3-dimethyl-1-propylindolin-2-ylidene)prop-1-en-1-yl)-3,3-dimethyl-3H-indol-1-ium-1-yl)hexanamido)-3-((2-((6-((2,5-dioxopyrrolidin-1-yl)oxy)-6-oxohexyl)(methyl)ammonio)ethyl)amino)-3-oxopropane-1-sulfonate 2,2,2-trifluoroacetate (8).

Compound **5** (6.3 mg, 0.0068 mmol, 1.0 eq) was stirred in dimethylformamide (0.6 mL) with *N*-hydroxysuccimide (8.6 mg, 0.075 mmol, 11 eq) under an inert atmosphere at ambient temperature. To the stirring solution was added *N,N'*-diisopropylcarbodiimide (9.5 μL, 0.061 mmol, 9.0 eq) in a dropwise fashion. The reaction mixture was stirred for 22h, after which the solvent was removed under lyophilization yielding crude product as a deep red oil. Purification which was preformed via reverse phase HPLC (40 to 70% B, 20mL/min, 40min, 530nm, R_t= 15-17min) afforded 3.3 mg (48% yield) of the TFA salt **8** as a deep red powder: FTIR: 1430, 1457, 1560, 1745, 2870, 2935, 2968, 3316 cm^{-1}; ^1H NMR (300MHz, CD_3OD): δ 1.08 (t, *J*=7.3, 2H), 1.44-2.03 (m, 26H), 2.28-2.32 (m, 2H), 2.66 (q, *J*=6.9 Hz, 2H), 2.81 (s, 2H), 2.83 (s, 2H), 2.95 (s, 3H), 3.00-3.25 (m, 4H), 3.38-3.77 (m, 4H), 4.13-4.17 (m, 4H), 4.67 (dd, *J*=

7.5, 5.1, 1H), 6.49 (d, *J*= 13.2 Hz, 1H), 6.52 (d, *J*= 13.2 Hz, 1H), 7.28-7.56 (m, 8H), 8.40-8.46 (m, 1H) (NH), 8.55 (t, *J*=13.5 Hz, 1H); ^{13}C NMR (75MHz, CD_3OD): δ 11.64, 22.06, 24.53, 25.17, 25.20, 26.29, 26.65, 26.70, 27.31, 28.33, 28.49, 31.40, 35.39, 35.45, 36.66, 36.68, 40.93, 41.00, 45.24, 46.80, 50.73, 50.77, 50.82, 52.04, 52.08, 53.16, 53.26, 57.31, 57.34, 57.57, 103.76, 104.01, 112.66, 112.70, 123.67, 126.89, 126.90, 130.12, 130.20, 142.33, 142.38, 143.53, 143.64, 152.33, 170.30, 171.99, 172.00, 173.69, 175.62, 175.64, 176.08, 176.35; HRMS (ESI): Exact mass calcd for $C_{48}H_{67}N_6O_9S$ $[M]^+$ 903.4685, found 903.4701.

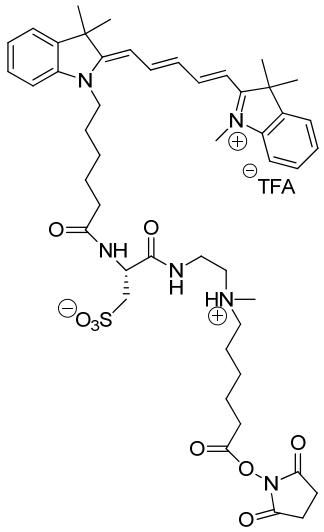

(2R)-2-(6-(3,3-dimethyl-2-((1E,3E)-5-((E)-1,3,3-trimethylindolin-2-ylidene)penta-1,3-dien-1-yl)-3H-indol-1-ium-1-yl)hexanamido)-3-((2-((6-((2,5-dioxopyrrolidin-1-yl)oxy)-6-oxohexyl)(methyl)ammonio)ethyl)amino)-3-oxopropane-1-sulfonate 2,2,2-trifluoroacetate (9).

Compound **6** (20.6mg, 0.022 mmol, 1.0 eq) was stirred in dimethylformamide (2.0 mL) with *N*-hydroxysuccimide (28.3 mg, 0.25 mmol, 11.0 eq) under an inert atmosphere at ambient temperature. To the stirring solution was added *N,N'*-

diisopropylcarbodiimide (31 μL, 0.19 mmol, 9.0 eq) in a dropwise fashion. The reaction mixture was stirred for 20h, after which the solvent was removed under lyophilization yielding the crude product as a deep blue oil. Purification whiched was preformed via reverse phase HPLC (60 to 90% B, 20mL/min, 30min, 600nm, R_t= 15-18min) provided 17.0 mg (76% yield) of the TFA salt **9** as a deep blue powder: FTIR: 1457, 1495, 1672, 1741, 2866, 2941, 3339 cm^{-1}; ^1H NMR (300MHz, CD_3OD): δ 1.47-1.56 (m, 4H), 1.73 (s, 12H), 1.77-1.83 (m,8H), 2.26-2.31 (m, 2H), 2.62-2.70 (m, 2H), 2.80 (s, 2H), 2.82 (s, 2H) 2.89 (s, 3H), 3.00-3.27 (m, 6H), 3.37-3.48 (m, 2H), 3.64 (s, 3H), 4.10 (t, 2H, *J*=7.2 Hz), 4.65-4.69 (m, 1H), 6.33-6.41 (m, 2H), 6.65-6.74 (m, 1H), 7.23-7.50 (m, 8H), 8.25 (dd, *J*=13.3, 13.2 Hz, 2H), 8.41-8.47 (m, 1H) (NH); ^{13}C NMR (75MHz, CD_3OD): δ 24.52, 24.58, 25.16, 25.23, 26.25 ,26.64, 26.74, 27.13, 27.17, 27.96, 28.12, 31.41, 31.78, 35.35, 35.43, 36.41, 40.93, 41.00, 44.97, 50.65, 52.12, 53.26, 53.34, 57.32, 57.35, 57.45, 57.63, 104.47, 104.81, 112.00, 112.17,123.43, 123.56, 126.34, 126.40, 126.86, 129.86, 129.94, 142.73, 142.79, 143.70,144.44, 155.64, 155.77, 170.27, 170.31, 171.98, 172.00, 173.74, 174.73, 175.59, 175.62; HRMS (ESI): Exact mass calcd for $C_{48}H_{65}N_6O_9S$ $[M]^+$ 901.4528, found 901.4553.

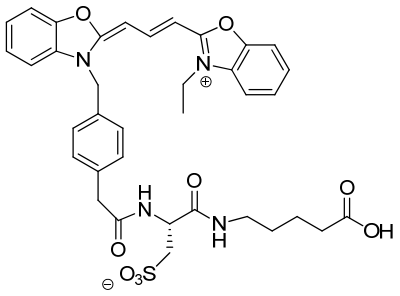

(R)-3-((4-carboxybutyl)amino)-2-(2-(4-((2-((1E,3Z)-3-(3-ethylbenzo[d]oxazol-2(3H)-ylidene)prop-1-en-1-yl)benzo[d]oxazol-3-ium-3-yl)methyl)phenyl)acetamido)-3-oxopropane-1-sulfonate (10).

2-[3-[3-[[4-[2-[(2,5-Dioxo-1-pyrrolidinyl)oxy]-2-oxoethyl]phenyl]methyl]-2(3H)-benzo-xazolylidene]-1-propenyl]-3-ethyl-benzoxazolium salt **1** (74.0 mg, 0.11 mmol, 1.0 eq) was stirred in dimethylformamide with the cysteic acid sidechain **XXXI** (149.4 mg, 0.56 mmol, 5.0 eq) under an inert atmosphere at ambient temperature. To the stirring solution was added 4-methylmorpholine (0.244 mL, 2.2 mmol, 20.0 eq) in a dropwise fashion. The reaction mixture was stirred for 18h, after which the solvent was removed under lyophilization yielding the crude product as a deep yellow oil. Purification which was preformed via reverse phase HPLC (30 to 70% B, 20mL/min, 30min, 450nm, R_t= 12.6-16.3min) afforded 51.0 mg (57% yield) of **10** as a deep yellow powder: FTIR: 1457, 1495, 1552, 1631, 1722, 2851, 2931, 3286; ^{1}H NMR (300MHz, CD_3OD): δ 1.42 (t, *J*=7.8, 3H)1.46-1.61 (m, 4H), 2.25 (t, *J*=6.6 Hz, 2H), 2.66 (s, 1H) (OH), 3.07-3.19 (m, 4H), 3.54-3.66 (m, 2H), 4.21 (q, *J*=6.9 Hz, 2H), 4.58 (dd, *J*= 8.1, 4.8Hz, 1H), 5.38 (s, 2H), 5.96 (d, *J*=13.2 Hz, 1H), 6.00 (d, *J*= 13.5Hz, 1H), 7.31-7.63 (m , 12H), 8.51 (dd, *J*=13.5, 13.2 Hz, 1H);; ^{13}C NMR (75MHz, DMSO-d_6): δ12.86, 21.75, 28.42, 33.26,

38.21, 41.87, 46.42, 50.97, 51.10, 52.19, 84.64, 86.08, 110.98, 111.05, 111.32, 111.43, 125.01, 125.25, 125.85, 126.00, 125.99, 127.08, 129.85, 130.80, 131.46, 132.03, 136.46, 146.36, 146.37, 146.46, 146.59, 161.57, 161.90, 169.39, 169.44, 170.42, 174.37; HRMS (ESI): Exact mass calcd for $C_{36}H_{39}N_4NaO_9S$ $[M+H]^+$ 725.2252, found 725.2260.

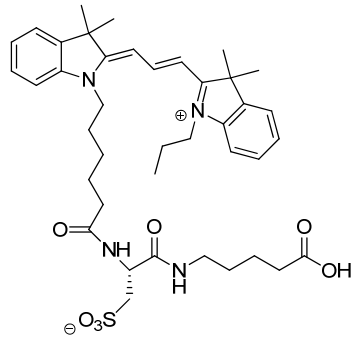

(R)-3-((4-carboxybutyl)amino)-2-(6-(2-((E)-3-((E)-3,3-dimethyl-1-propylindolin-2-ylidene)prop-1-en-1-yl)-3,3-dimethyl-3H-indol-1-ium-1-yl)hexanamido)-3-oxopropane-1-sulfonate (11).

2-[3-(1,3-Dihydro-3,3-dimethyl-1-propyl-2H-indol-2-ylidene)-1-propenyl]-1-[6-[(2,5-di-oxo-1-pyrro-lidinyl)oxy]-6-oxohexyl]-3,3-dimethyl-3H-indolium salt **2** (15.5 mg, 0.022 mmol, 1.0 eq) was stirred in dimethylformamide (1.6 mL) with the cysteic acid sidechain **XXXI** (50.3 mg, 0.11 mmol, 5.0 eq) under an inert atmosphere at ambient temperature. To the stirring solution was added 4-methylmorpholine (0.048 mL, 0.44 mmol, 20.0 eq) in a dropwise fashion. The reaction mixture was stirred for 17h, after which the solvent was removed under lyophilization yielding the crude product as a deep red oil. Purification which was preformed via reverse phase HPLC (40 to 80% B, 20mL/min, 30min, 530nm, R_t= 12.1-15.6min) provided 15.9 mg (57% yield) of **11** as a deep red powder: FTIR: 1429, 1460, 1559, 1662, 1730, 2867, 2932, 2973, 3304 cm^{-1}; ^1H NMR

(300MHz, CD_3OD): δ 1.07 (t, *J*=7.2 Hz, 2H), 1.47-1.67 (m, 6H), 1.77 (s, 12H), 1.82-1.94 (m, 6H), 2.27-2.43 (m, 4H), 3.13-3.25 (m, 4H), 4.12-4.19 (m, 4H), 4.65 (dd, *J*=8.7, 3.9 Hz, 1H), 6.58 (d, *J*=13.2 Hz, 1H), 6.61 (d, *J*=13.2 Hz, 1H), 7.27-7.45 (m, 6H), 7.52-7.54 (m, 2H), 8.54 (t, *J*=13.2 Hz, 1H); ^{13}C NMR (75MHz, CD_3OD): δ 11.66, 22.10, 23.34, 23.42, 26.31, 26.99, 28.26, 28.51, 29.82, 29.88, 34.44, 34.61, 36.69, 40.24, 40.30, 45.38, 46.76, 50.74, 52.76, 52.99, 104.04, 104.23, 112.67, 112.72, 123.57, 123.61, 126.77, 126.79, 130.09, 130.20, 142.38, 142.40, 143.51, 143.73, 152.41, 172.93, 176.04, 176.05, 176.23, 177.39; HRMS (ESI): Exact mass calcd for $C_{40}H_{55}N_4O_7S$ $[M+H]^+$ 735.3786 found 735.3800.

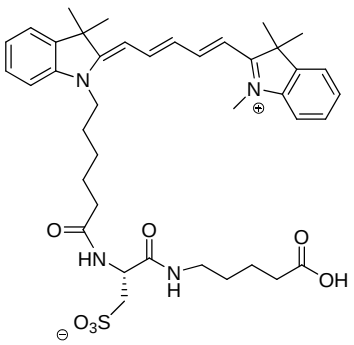

(R)-3-((4-carboxybutyl)amino)-2-(6-(3,3-dimethyl-2-((1E,3E)-5-((E)-1,3,3-trimethylindolin-2-ylidene)penta-1,3-dien-1-yl)-3H-indol-1-ium-1-yl)hexanamido)-3-oxopropane-1-sulfonate (12).

2-[5-(1,3-Dihydro-1,3,3-trimethyl-2H-indol-2-ylidene)-1,3-pentadienyl]-1-[6-[(2,5-dioxo-1-pyrrolidi-nyl)oxy]-6-oxohexyl]-3,3-dimethyl-3H-indolium salt **3** (22.2 mg, 0.032 mmol, 1.0 eq) was stirred in dimethylformamide (2.3 mL) with the cysteic acid sidechain **XXXI** (42.9 mg, 0.16 mmol, 5.0 eq) under an inert atmosphere at ambient

temperature. To the stirring solution was added 4-methylmorpholine (0.070 mL, 0.64 mmol, 20.0 eq) in a dropwise fashion. The reaction mixture was stirred for 22h, after which the solvent was removed under lyophilization yielding the crude product as a deep blue oil. Purification which was preformed via reverse phase HPLC (50 to 90% B, 20mL/min, 30min, 600nm, R_t= 8.4-9.9min) provided 12.6 mg (52% yield) of **12** as a deep blue powder: FTIR: 1336, 1375, 1461, 1480, 1495, 1654, 1722, 2862, 2935, 3059, 3316; ^{1}H NMR (300MHz, CD_3OD): δ 1.50-1.64 (m, 6H), 1.70 (s, 12H), 1.76-1.83 (m, 4H), 2.24-2.37 (m, 4H), 3.15-3.23 (m, 4H), 3.62 (s, 3H), 4.10 (t, *J*=7.2 Hz, 2H), 4.66 (dd, *J*=8.4, 4.2 Hz, 1H), 6.32 (d, *J*=13.3 Hz, 1H), 6.35 (d, *J*=13.3 Hz, 1H), 6.75 (t, *J*=12.9 Hz, 1H), 7.22-7.48 (m, 8H), 8.20 (dd, *J*= 13.3, 12.9 Hz, 2H); ^{13}C NMR (75MHz, CD_3OD): δ 23.34, 23.42, 26.21, 27.13, 27.99, 28.09, 28.16, 29.81, 29.87, 31.67, 34.44, 34.61, 36.70, 40.25, 40.31, 44.98, 50.50, 50.63, 52.82, 52.90, 104.74, 111.87, 112.29, 123.37, 123.47, 126.21, 126.31, 127.22, 129.82, 129.96, 142.66, 142.82, 143.68, 144.50, 155.50, 155.60, 172.91, 174.73, 174.75, 175.18, 175.94, 177.38; HRMS (ESI): Exact mass calcd for $C_{40}H_{52}N_4NaO_7S$ $[M+Na]^+$ 755.3449, found 755.3455.

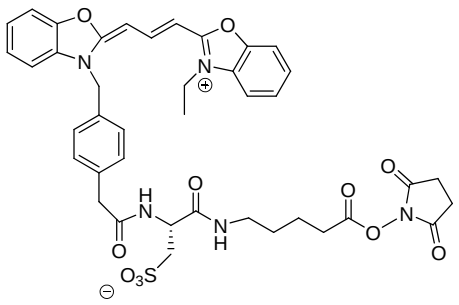

(R)-3-((5-((2,5-dioxopyrrolidin-1-yl)oxy)-5-oxopentyl)amino)-2-(2-(4-((2-((1E,3Z)-3-(3-ethylbenzo[d]oxazol-2(3H)-ylidene)prop-1-en-1-yl)benzo[d]oxazol-3-ium-3-yl)methyl)phenyl)acetamido)-3-oxopropane-1-sulfonate (13).

Compound **10** (12.60 mg, 0.018 mmol, 1.0 eq) was stirred in dimethylformamide (1.6 mL) with *N*-hydroxysuccimide (26.80 mg, 0.23 mmol, 13.0 eq) under an inert atmosphere at ambient temperature. To the stirring solution was added *N,N'*-diisopropylcarbodiimide (30 μL, 0.19 mmol, 11.0 eq) in a dropwise fashion. The reaction mixture was stirred for 18h, after which the solvent was removed under lyophilization yielding the crude product as a deep yellow oil. Purification which was preformed via reverse phase HPLC (30 to 70% B, 20mL/min, 40min, 450nm, R_t= 22.5-23.0min) provided 6.3 mg (43% yield) of **13** as a deep yellow powder: FTIR: 1465, 1510, 1563, 1635, 1737, 2927, 3297; ^{1}H NMR (500MHz, CD_3OD): δ 1.41 (t, 3H, *J*=7.5 Hz), 1.51-1.56 (m, 2H), 1.63-1.69 (m, 2H), 2.57 (t, *J*=7.5 Hz, 2H), 2.79 (s, 4H), 3.09-3.19 (m, 4H), 3.56-3.63 (m ,2H), 4.21 (q, *J*=7.5 Hz, 2H), 4.58 (dd, $J_=$ 8.5, 4.5 Hz, 1H), 5.38 (s, 2H), 5.95 (d, *J*= 13.5Hz, 1H), 5.98 (d, *J*=13.5 Hz, 1H), 7.32-7.88 (m, 12H), 8.51 (t, *J*=13.5 Hz, 1H); ^{13}C NMR (125MHz, CD_3OD): δ 13.40, 23.01, 26.64, 29.37, 31.30, 39.89, 40.63, 43.39, 48.24, 52.61, 53.07, 86.13, 86.18, 87.03, 87.08, 112.00, 112.14, 112.24, 112.38, 126.51, 126.77, 127.40, 127.48, 128.78, 131.57, 132.38, 133.04, 133.80, 137.43, 148.48, 148.66, 149.03, 149.11, 149.20, 163.73, 164.18, 170.32, 171.94, 172.72, 173.60; HRMS (ESI): Exact mass calcd for $C_{40}H_{42}N_5O_{11}S$ $[M+H]^+$ 800.2596, 800.2581.

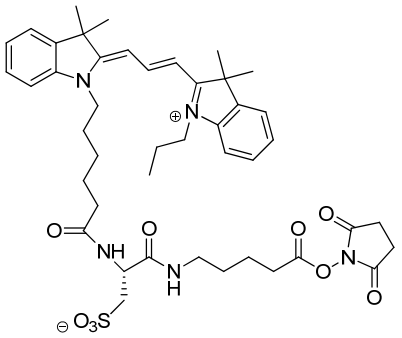

(R)-2-(6-(2-((E)-3-((E)-3,3-dimethyl-1-propylindolin-2-ylidene)prop-1-en-1-yl)-3,3-dimethyl-3H-indol-1-ium-1-yl)hexanamido)-3-((5-((2,5-dioxopyrrolidin-1-yl)oxy)-5-oxopentyl)amino)-3-oxopropane-1-sulfonate (14).

Compound **11** (61.9 mg, 0.084 mmol, 1.0 eq) was stirred in dimethylformamide (7.6 mL) with *N*-hydroxysuccimide (126.0 mg, 1.1 mmol, 13.0 eq) under an inert atmosphere at ambient temperature. To the stirring solution was added *N,N'*-diisopropylcarbodiimide (0.81 mL, 0.93 mmol, 11.0 eq) in a dropwise fashion. The reaction mixture was stirred for 20h, after which the solvent was removed under lyophilization yielding the crude product as a deep red oil. Purification which was preformed via reverse phase HPLC (40 to 80% B, 20mL/min, 40min, 530nm, R_t = 16.6-18.5min) provided 40 mg (54% yield) of **14** as a deep red powder: FTIR: 1427, 1456, 1559, 1665, 1737, 1775, 2972, 2935, 3317; ^{1}H NMR (300MHz, CD_3OD): δ 1.07 (t, *J*= 7.2 Hz, 3H), 1.55-1.72 (m, 4H), 1.76 (s, 12H), 1.82-1.98 (m,8), 2.22-2.42 (m, 2H), 2.65 (t, *J*= 6.9 Hz, 2H), 2.79 (s, 4H), 3.11-3.27 (m, 4H), 4.12-4.19 (m, 4H), 4.65 (dd, *J*= 9.0, 4.2 Hz, 1H), 6.58 (d, *J*=13.5, 1H), 6.61 (d, *J*=13.2, 1H), 7.27-7.46 (m, 6H), 7.52-7.54 (m, 2H), 8.54 (dd, *J*=13.5, 13.2 Hz, 1H); ^{13}C NMR (75MHz, CD_3OD): δ 11.68, 18.52, 22.09, 23.08, 26.30, 26.63, 27.00, 28.24, 28.47, 28.51, 29.47, 31.33, 36.68, 39.95, 45.39, 46.76,

50.72, 52.74, 53.03, 58.47, 103.99, 104.03, 104.22, 112.66, 112.71, 123.58, 123.61, 126.77, 126.79, 126.85, 130.08, 130.19, 142.37, 142.39, 143.50, 143.71, 152.37, 170.31, 171.92, 172.93, 172.99, 176.01, 176.03, 176.21; HRMS (ESI): Exact mass calcd for $C_{44}H_{58}N_5O_9S$ $[M+H]^+$ 832.3950, found 832.3935.

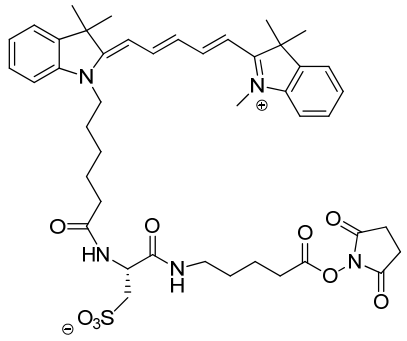

(R)-2-(6-(3,3-dimethyl-2-((1E,3E)-5-((E)-1,3,3-trimethylindolin-2-ylidene)penta-1,3-dien-1-yl)-3H-indol-1-ium-1-yl)hexanamido)-3-((5-((2,5-dioxopyrrolidin-1-yl)oxy)-5-oxopentyl)amino)-3-oxopropane-1-sulfonate (15).

Compound **12** (28.4 mg, 0.038 mmol, 1.0 eq) was stirred in dimethylformamide (3.5 mL) with *N*-hydroxysuccimide (58.0 mg, 0.50 mmol, 13.0 eq) under inert atmosphere and at ambient temperature. To the stirring solution was added *N,N'*-diisopropylcarbodiimide (0.065 mL, 0.42 mmol, 11.0 eq) in a dropwise fashion. The reaction mixture was stirred for 18h, after which the solvent was removed under lyophilization yielding the crude product as a deep blue oil. Purification which was preformed via reverse phase HPLC (50 to 80% B, 20mL/min, 40min, 600nm, R_t= 10.4-11.7min) afforded 21.6 mg (69% yield) of **15** as a deep blue powder: FTIR: 1336, 1371, 1454, 1483, 1495, 1657, 1733, 1786, 2870, 2938, 3316; ^{1}H NMR (500MHz, CD_3OD): δ 1.49-1.66 (m, 6H), 1.71 (s, 12H),1.74-1.84 (m, 4H), 2.25-2.37 (m, 2H), 2.64 (t, *J*=7.5 Hz,

2H), 2.79 (s, 4H), 3.15-3.26 (m, 4H), 3.62 (s, 3H), 4.10 (t, *J*=3.5 Hz, 2H), 4.66 (dd, *J*=8.5, 3.5 Hz, 1H), 6.35 (t, *J*=13.0 Hz, 2H), 6.78 (t, *J*=12.5 Hz, 1H), 7.22-7.32 (m, 4), 7.37-7.40 (m, 2), 7.45-7.47 (m, 2), 8.22 (dd, *J*=13.0, 12.5 Hz, 2H); ^{13}C NMR (125MHz, CD_3OD): δ 23.11, 26.17, 26.64, 27.15, 28.02, 28.12, 29.47, 31.35, 31.73, 36.72, 39.98, 45.05, 50.54, 50.65, 52.82, 52.97, 104.75, 111.89, 112.30, 123.35, 123.46, 126.23, 126.31, 127.21, 129.81, 129.94, 142.65, 142.89, 143.68, 143.71, 144.51, 155.42, 155.48, 155.58, 170.31, 171.82, 171.86, 171.92, 172.91, 172.98, 174.78, 175.26,175.30, 175.91; HRMS (ESI): Exact mass calcd for $C_{44}H_{55}N_5NaO_9S$ $[M+Na]^+$ 852.3613, found 852.3605.

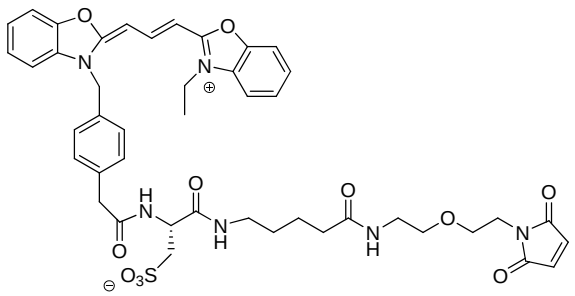

(R)-3-((5-((2-(2-(2,5-dioxo-2,5-dihydro-1H-pyrrol-1-yl)ethoxy)ethyl)amino)-5-oxopentyl)amino)-2-(2-(4-((2-((1E,3Z)-3-(3-ethylbenzo[d]oxazol-2(3H)-ylidene)prop-1-en-1-yl)benzo[d]oxazol-3-ium-3-yl)methyl)phenyl)acetamido)-3-oxopropane-1-sulfonate (16).

Compound **13** (13.5 mg, 0.017 mmol, 1.0 eq) was stirred in dimethylformamide (1.2 mL) with *N*-(5-amino-3-oxapentyl) maleimide trifluoroacetate (25.2 mg, 0.084 mmol, 5.0 eq) under an inert atmosphere at ambient temperature. To the stirring solution was added 4-methylmorpholine (0.040 mL, 0.34 mmol, 20.0 eq) in a dropwise fashion. The reaction mixture was stirred for 20h, after which the solvent was removed under

lyophilization yielding the crude product as a deep yellow oil. Purification which was performed via reverse phase HPLC (30 to 70% B, 20mL/min, 40min, 450nm, R_t= 18.6-19.6min) afforded 5.6 mg (38% yield) of **17** as a deep yellow powder: FTIR: 1460, 1506, 1559, 1635, 1711, 2856, 2938, 3082, 3290 cm^{-1}; ^1H NMR (500MHz, CD_3OD): δ 1.44-1.48 (m, 5H), 1.56-1.60 (m, 2H), 2.14 (t, *J*=7.5 Hz, 3H), 3.10-3.16 (m, 2H), 3.24-3.26 (m, 2H), 3.45-3.47 (m, 2H), 3.55-3.66 (m, 8H), 4.25 (q, *J*=7.5 Hz, 2H), 4.57-4.61 (m, 1H), 5.40 (s, 2H), 5.98 (d, *J*= 13.5 Hz, 1H), 6.03 (d, *J*= 13.5 Hz, 1H), 6.8 (s, 2H), 7.31-7.65 (m, 12H), 7.81-7.85 (m, 1H) (NH), 7.95-7.98 (m, 1H) (NH), 8.18-8.20 (m, 1H) (NH), 8.55 (t, *J*=13.5 Hz, 1H); ^{13}C NMR (125MHz, DMSO-d_6): δ 12.80, 22.52, 28.45, 34.88, 36.70, 38.26, 38.31, 40.42, 41.86, 46.41, 51.04, 52.19, 52.24, 66.73, 68.58, 84.57, 84.63, 85.99, 86.06, 110.93, 111.00, 111.28, 111.38, 124.97, 125.21, 125.92, 125.97, 127.04, 129.80, 130.75, 131.41, 131.97, 134.50, 136.41, 146.29, 146.37, 146.43, 146.55, 161.55, 161.88, 169.43, 170.34, 170.87, 172.03; HRMS (ESI): Exact mass calcd for $C_{44}H_{49}N_6O_{11}S$ $[M+H]^+$ 869.3175, found 869.3208.

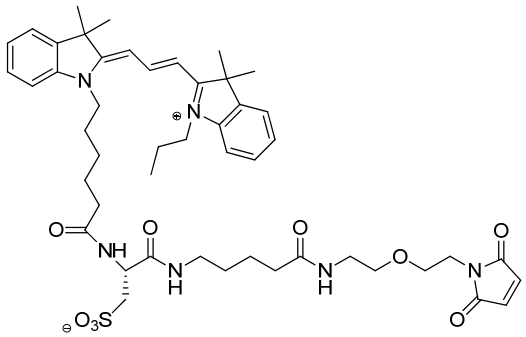

(R)-2-(6-(2-((E)-3-((E)-3,3-dimethyl-1-propylindolin-2-ylidene)prop-1-en-1-yl)-3,3-dimethyl-3H-indol-1-ium-1-yl)hexanamido)-3-((5-((2-(2-(2,5-dioxo-2,5-dihydro-1H-pyrrol-1-yl)ethoxy)ethyl)amino)-5-oxopentyl)amino)-3-oxopropane-1-sulfonate (17).

Compound **14** (37.3 mg, 0.045 mmol, 1.0 eq) was stirred in dimethylformamide (3.2 mL) with *N*-(5-amino-3-oxapentyl) maleimide trifluoroacetate (66.8 mg, 0.22 mmol, 5.0 eq) under an inert atmosphere at ambient temperature. To the stirring solution was added 4-methylmorpholine (0.098 mL, 0.89 mmol, 20.0 eq) in a dropwise fashion. The reaction mixture was stirred for 17h, after which the solvent was removed under lyophilization yielding the crude product as a deep red oil. Purification which was performed via reverse phase HPLC (40 to 80% B, 20mL/min, 40min, 530nm, R_t= 15-16.4min) afforded 17.6 mg (54% yield) of **18** as a deep red powder: FTIR: 1430, 1456, 1556, 1658, 1711, 2866, 2935, 2968, 3074, 3394 cm^{-1}; ^1H NMR (300MHz, CD_3OD): δ 1.07 (t, *J*=7.5 Hz, 3H), 1.52-1.67 (m, 6H), 1.77 (s, 12H), 1.83-1.93 (m, 6H) 2.20 (t, *J*= 6.3, 2H), 2.24-2.42 (m, 2), 3.12-3.27 (m, 6), 3.47-3.51 (m, 2H), 3.57-3.60 (m, 2H), 3.65-3.69 (m, 2H), 4.12-4.19 (m, 4), 4.65 (dd, *J*=9.0, 4.5 Hz, 1H), 6.56 (d, *J*=13.5 Hz, 1H), 6.61 (d, *J*=13.2 Hz, 1H), 6.82 (s, 2), 7.27-7.47 (m, 6), 7.50-7.54 (m,2) 8.54 (dd, *J*=13.5, 13.2 Hz, 1H); ^{13}C NMR (75MHz, CD_3OD): δ 11.67, 18.52, 22.10, 24.33, 26.32, 27.02, 28.27, 28.48, 28.51, 29.80, 36.66, 36.72, 38.31, 40.27, 40.44, 45.38, 46.77, 50.74, 52.76, 52.98, 58.47, 68.92, 70.17, 104.03, 104.22, 112.67, 112.72, 123.58, 123.61, 126.78, 126.80, 130.09, 130.21, 135.64, 142.37, 142.40, 143.51, 143.71, 152.33, 152.39, 159.83, 160.35, 172.66, 172.90, 175.97, 176.05, 176.20, 176.23; HRMS (ESI): Exact mass calcd for $C_{48}H_{64}N_6NaO_9S$ $[M+Na]^+$ 923.4348, found 923.4345.

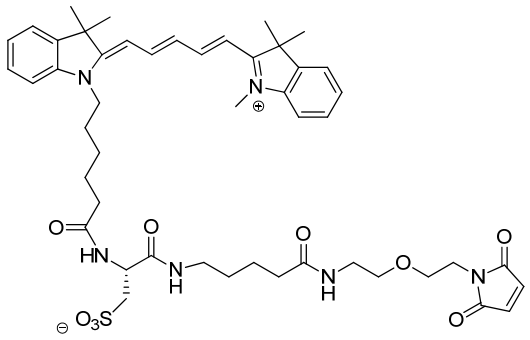

(R)-2-(6-(3,3-dimethyl-2-((1E,3E)-5-((E)-1,3,3-trimethylindolin-2-ylidene)penta-1,3-dien-1-yl)-3H-indol-1-ium-1-yl)hexanamido)-3-((5-((2-(2-(2,5-dioxo-2,5-dihydro-1H-pyrrol-1-yl)ethoxy)ethyl)amino)-5-oxopentyl)amino)-3-oxopropane-1-sulfonate (18).

Compound **15** (14.0 mg, 0.016 mmol, 1 eq) was stirred in dimethylformamide (1.1 mL) with *N*-(5-amino-3-oxapentyl) maleimide trifluoroacetate (25.2 mg, 0.22 mmol, 5.0 eq) under inert atmosphere and at ambient temperature. To the stirring solution was added 4-methylmorpholine (0.030 mL, 0.32 mmol, 20.0 eq) in a dropwise fashion. The reaction mixture was stirred for 18h, after which the solvent was removed under lyophilization yielding the crude product as a deep blue oil. Purification which was performed via reverse phase HPLC (40 to 70% B, 20mL/min, 40min, 600nm, R_t = 17.3-18.5min) provided 7.0 mg (45% yield) of **19** as a deep blue powder: FTIR: 1460, 1499, 1476, 1662, 1707, 2862, 2927, 2984, 3294 cm^{-1}; ^1H NMR (500MHz, CD_3OD): δ 1.49-1.66 (m, 4H), 1.72(s, 12H), 1.75-1.85 (m, 6H), 2.20 (t, *J*=7.5 Hz, 2H), 2.25-2.37 (m, 2H), 3.15-3.29 (m, 6H), 3.49 (t, *J*=5.5 Hz, 2H), 3.58 (t, *J*=5.5 Hz, 2H), 3.63 (s, 3H), 3.67 (t, *J*=5.5 Hz, 2H), 4.11 (t, 2H, *J*=7.0 Hz), 4.66 (dd, *J*=9.0, 4.5 Hz, 1H), 6.35 (t, *J*=11.0 Hz, 2H), 6.76 (t, *J*=12.5 Hz, 1H), 6.82 (s, 2H), 7.23-7.31 (m, 4H), 7.38-7.42 (m, 2H), 7.45-7.48 (m, 2H), 8.21 (dd, *J*=12.5, 11.0 Hz, 2H); ^{13}C NMR (125MHz, CD_3OD): δ 24.33,

26.19, 27.18, 28.02, 28.12, 28.17, 29.79, 31.71, 36.69, 36.75, 38.35, 40.28, 40.44, 45.01, 50.52, 50.69, 52.84, 52.93, 68.95, 70.21, 104.32, 104.52, 104.79, 104.79, 111.95, 112.35, 123.37, 123.47, 126.24, 126.34, 127.12, 129.83, 129.96, 135.63, 142.68, 142.82, 143.69, 144.50, 155.45, 155.50 155.55, 155.59, 172.88, 174.74, 174.76, 175.28, 175.33, 175.88, 176.20; HRMS (ESI): Exact mass calcd for $C_{48}H_{63}N_6O_9S$ $[M+H]^+$ 899.4372, found 899.4387.

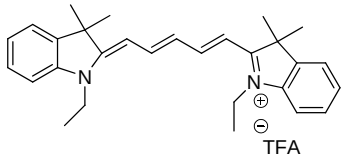

1-ethyl-2-((1E,3E)-5-((E)-1-ethyl-3,3-dimethylindolin-2-ylidene)penta-1,3-dien-1-yl)-3,3-dimethyl-3H-indol-1-ium 2,2,2-trifluoroacetate (21).

To a round bottom flask charged with absolute ethanol (135 mL) and equipped with a stir bar, 1-ethyl-2,3,3-trimethyl-3H-indolium bromide (460.0 mg, 1.7 mmol, 1.0 eq) and 2-(4-Phenylamino-1E,3E-butadien-1-yl)-1-ethyl-3,3-dimethylindolium chloride (605.0mg, 1.7 mmol, 1.0 eq). To the reaction mixture was added sodium acetate (168 mg, 2.1 mmol, 1.2 eq) and the reaction mixture was refluxed under inert atmosphere for 3.5 h. The solvent was removed via rotary evaporation followed by drying under lyophilization yielding the crude product as a deep blue oil. Purification which was preformed via reverse phase HPLC (40 to 70% B, 20 mL/min, 40 min, 600 nm, R_t = 29-36 min) afforded 63.3 mg (5% yield) of TFA salt of **12** as a deep blue powder: FTIR: 1453, 1486, 1570, 1684, 1723, 2878, 2969 cm^{-1}; ^1H NMR (500MHz, CD_3OD): δ 1.38 (t, *J*=7.5, 6H), 1.71 (s, 12H), 4.14 (q, *J*=7.5, 4H), 6.27 (d, 2H, *J*=13.5), 6.62 (t, J=12.5, 1H), 7.24-7.39 (m, 4H), 7.41-7.42 (m, 2H), 7.48-7.49 (m, 2H), 8.24 (dd, *J*=13.5, 12.5, 2H); ^{13}C NMR

(125 MHz, CD_3OD): δ 12.65, 28.00, 40.09, 50.71, 104.07, 111.91, 123.57, 126.41, 126.64, 129.92, 142.93, 143.23, 155.72, 174.50; HRMS (ESI): Exact mass calcd for $C_{29}H_{35}N_2$ $[M]^+$ 411.2795, found 411.2812.

APPENDIX B

Z-Cy3 VS. Cy3 DIGE FLUOR: SPOT VOLUME COMPARISON

					% difference
Ref. Spot	Z-Cy3 Volume	Norm. Vol. Z-Cy3	Cy3 Volume	Norm. Vol. Cy3	(Z-Cy3/Cy3)*100
26	861707.8053	1.39899584	621593.3874	0.801376868	174.5740231
14	9913523.991	1.285761017	6549322.488	0.739512572	173.8660119
43	2722525.263	3.021152248	1992216.39	1.918049868	157.5116632
44	428956.3146	1.542807765	313095.7698	0.988827934	156.0238857
69	2007832.184	1.021938981	1467509.953	0.701245294	145.7320269
123	22248088.64	1.065655954	14817539.06	0.737940983	144.409374
80	7498286.994	1.208396881	6017404.394	0.849708193	142.213161
82	1381192.879	1.112439678	1129199.441	0.787215994	141.3131448
100	13446759.62	1.111984149	9700188.064	0.793888689	140.0680176
102	1284024.135	1.029829651	1268868.913	0.740270451	139.115326
92	2297298.703	0.992025268	2190641.993	0.715545472	138.6390253
138	476582.7532	1.115050245	561375.3223	0.809347261	137.7715472
112	1062732.088	1.059212721	1337674.988	0.76971907	137.6102999
189	23372941.33	1.045051069	22461048.47	0.770930322	135.5571365
104	12336159.9	1.056903516	9840768.988	0.782673537	135.0375944
142	47415303.53	0.995535818	33827636.52	0.739053446	134.704171
85	4900018.181	1.160210622	4617069.497	0.862172145	134.568326
119	13653867.77	1.131863791	12511778.75	0.842513108	134.3437603
215	1914824.075	0.943796159	1884460.511	0.705233419	133.8274865
114	1324272.961	1.10427523	1258456.434	0.825236646	133.8131596
77	1071244.453	0.894986603	972586.158	0.673269146	132.9314746
157	746867.3583	1.051250168	836982.9477	0.790873818	132.9226161
205	440252.1874	0.974948726	490788.7943	0.734928576	132.6589763
116	2158356.003	1.005168307	1940915.855	0.758544162	132.5128262
159	877994.0728	0.927570271	883020.1753	0.708036997	131.0059044
117	1514098.793	0.873885263	1604619.813	0.668561242	130.7113259
253	3148583.705	1.361829426	3138758.796	1.042525323	130.6279469
127	4886982.246	0.860394518	4649713.614	0.660958658	130.1737269
113	2372780.395	0.992258674	2840314.504	0.763283305	129.9987394
243	166572.7805	0.888935204	190341.3389	0.685455261	129.6853718
154	4637899.921	1.238079544	6164850.804	0.955673429	129.5504831
206	3569977.964	0.949268448	4091790.936	0.733377097	129.4379729
203	1148714.617	0.939479649	1218980.107	0.728228992	129.0088226
263	7074902.707	1.060833083	6871391.523	0.822450978	128.9843542
132	1959133.361	1.022130082	1627410.627	0.792768312	128.931753
					% difference

Ref. Spot	Z-Cy3 Volume	Norm. Vol. Z-Cy3	Cy3 Volume	Norm. Vol. Cy3	(Z-Cy3/Cy3)*100
134	2565952.921	1.087543309	2839851.839	0.845486976	128.6292208
406	1499567.764	1.541400483	1279521.531	1.198922417	128.5654902
137	1034455.559	0.916730454	1194360.544	0.713976046	128.3979286
186	5789340.21	1.065420078	4858089.435	0.829987153	128.3658518
191	72841773.76	1.026782567	57500661.54	0.800009953	128.346224
99	734978.2196	0.976773696	859371.7478	0.765080256	127.6694424
392	1161588.333	1.060155486	1157318.345	0.831695452	127.4691936
271	14107411.2	1.094048507	12742081.33	0.858970692	127.3673848
169	5096891.518	1.091029928	4728082.925	0.857693152	127.205158
143	47854509.33	1.074031923	52300029.43	0.847131409	126.784571
136	2208890.45	0.962252222	2567101.868	0.764861327	125.8074095
71	1670502.462	1.037896948	1362118.441	0.826423377	125.5890112
139	3904183.834	1.054086728	3651355.654	0.841504986	125.2620895
204	3017854.328	0.921372832	3627010.349	0.735632323	125.2490958
190	1266026.242	0.805431608	1556295.821	0.644814896	124.9089643
166	3196494.789	0.788992558	2873939.243	0.632315546	124.7782952
226	66686705.44	0.992650358	70750827.85	0.796716281	124.5927041
224	2318023.85	0.878160367	2702623.689	0.705118912	124.540748
197	11937564.75	0.870286807	11751913.98	0.701021258	124.1455658
467	610167.0545	1.004234391	748301.1676	0.811988264	123.6759737
165	2008818.352	0.991519959	2386691.659	0.802415628	123.5668803
188	1605288.134	1.186844945	2147379.274	0.960717194	123.5373898
184	806955.3537	0.876947625	863551.4944	0.711347543	123.2797714
272	19578580.15	0.990807013	17366126.96	0.804341296	123.1824125
147	10500137.36	0.948229412	10578637.38	0.769870758	123.1673501
162	17996729.79	0.9728501	23923974.64	0.789949317	123.1534833
201	835939.366	0.87759782	1026549.856	0.712898983	123.1026892
294	12619405.8	1.002625243	13867098.21	0.814943833	123.029981
125	2825617.695	0.96732091	4230366.207	0.786497093	122.9910343
256	3768432.6	1.111493273	4440792.827	0.905508566	122.7479579
163	5140472.995	0.982819016	4881757.01	0.801470128	122.6270301
298	2029158.504	1.030214929	2239404.896	0.84155361	122.4182176
279	4614613.208	1.001586386	4544651.646	0.818375387	122.387159
84	3209836.877	1.08439011	3048011.741	0.886697075	122.2954423
249	1867108.322	0.819462595	1321140.693	0.670616366	122.1954364
181	8103846.003	1.046801876	8005958.932	0.856832185	122.1711666
221	972416.0199	0.978782402	1045439.392	0.801796866	122.0736129
					% difference

Ref. Spot	Z-Cy3 Volume	Norm. Vol. Z-Cy3	Cy3 Volume	Norm. Vol. Cy3	(Z-Cy3/Cy3)*100
172	2084284.122	0.937794468	1789088.94	0.769091163	121.9354106
161	4619418.401	1.004220541	5052901.452	0.825194172	121.6950597
228	2641522.21	0.976432158	3359106.273	0.802965475	121.6032555
185	1117534.569	0.969176276	1361186.305	0.797091613	121.5890696
237	941270.8333	0.860613684	627192.1292	0.707884077	121.5755111
150	2197527.616	0.942276791	2452828.966	0.775537033	121.4999092
232	1185465.913	0.916850081	1831225.665	0.754736774	121.4794498
234	621097.9721	0.872966702	974414.344	0.719168543	121.3855514
199	3818719.292	0.92917435	3887833.169	0.7669147	121.1574573
262	2180073.481	0.953097087	1937842.21	0.788039408	120.9453585
198	1633454.684	0.993738853	1961923.88	0.821904057	120.9069166
236	657805.2029	0.908177658	730102.7378	0.752893721	120.6249478
257	3782683.228	0.965226395	3721720.652	0.800726759	120.5437915
319	4554905.293	0.992942081	4071283.861	0.82422454	120.4698517
194	2805634.931	0.881620209	3628907.69	0.732059338	120.4301568
187	923776.572	0.874203973	1302523.581	0.726087578	120.3992464
440	1710252.737	1.286600011	1761130.649	1.069716873	120.274817
248	7594428.663	0.873760928	9438289.049	0.726673566	120.2411879
175	2056552.396	0.944416848	2347794.787	0.785606791	120.2149546
211	13134255.98	0.863014669	14536000.49	0.718619369	120.0934328
275	43540253.58	0.957587443	41807274.99	0.798301022	119.9531777
216	12353506.09	1.147783665	17745201.37	0.957321839	119.8952765
246	3153565.346	1.071124147	3803470.815	0.895642379	119.5928389
210	1635383.661	0.975449722	2029155.449	0.815983296	119.5428541
437	801619.4499	0.961317526	837146.6275	0.805477989	119.3474607
167	723785.5299	1.037835966	817925.5399	0.869816921	119.3165988
247	1925301.793	0.972471395	2417948.306	0.8151553	119.2989108
218	8249642.206	1.075566355	10395632.3	0.90434139	118.9336645
135	4149886.741	0.864911862	3904798.281	0.72771719	118.8527458
229	14627442.98	0.951409002	14039218.7	0.801149022	118.7555593
168	399305.7673	0.818587244	600124.4488	0.689798266	118.670528
260	11083406.63	0.926638981	13471174	0.78098472	118.6500781
487	312178.1151	0.927797551	424137.7718	0.782497953	118.5686874
202	4978217.635	0.867605915	6116418.987	0.732201382	118.4927995
233	7244689.609	0.889690091	9350598.729	0.751846139	118.3340639
225	2578063.92	0.952894852	2666787.822	0.806210822	118.1942521
273	1290503.803	0.793591442	1607271.507	0.672326756	118.0365699
					% difference

Ref. Spot	Z-Cy3 Volume	Norm. Vol. Z-Cy3	Cy3 Volume	Norm. Vol. Cy3	(Z-Cy3/Cy3)*100
266	113324090.1	1.12275116	130803387.4	0.952206595	117.9104583
334	878342.9978	0.905942845	993738.7422	0.768724081	117.8501971
126	2593327.307	0.852328969	2536377.256	0.72326897	117.8439838
131	153144.695	1.121981746	186185.2954	0.952226968	117.827134
239	15579179.89	0.953540699	17163227.59	0.809931579	117.7310188
283	34681979.38	0.916602851	32266605.91	0.781227021	117.3286158
245	5855407.272	1.007728853	8227414.856	0.859160734	117.292238
337	8409309.253	1.024725482	10182093.43	0.873818265	117.2698629
494	651462.2788	0.899886365	846059.5343	0.769189633	116.9914839
250	1207299.366	0.929851382	1449509.04	0.795688032	116.8613005
183	13451661.83	0.885920114	14491828.15	0.759463887	116.6507228
193	1027978.399	0.855333891	1200086.419	0.735130389	116.3513172
220	10432223.86	0.917243605	10715007.72	0.788355617	116.3489655
223	1386539.097	0.822680486	1624261.041	0.707706881	116.2459357
478	915173.3952	1.336949603	688701.4607	1.153574017	115.8962999
230	23389717.08	1.002443726	32010395.61	0.867052803	115.6150725
280	1941325.474	0.961829796	2658725.498	0.832089295	115.5921368
231	2070158.503	0.860522275	2636253.932	0.744650534	115.5605529
291	2823455.113	0.991728845	3927149.416	0.859051849	115.4445854
242	1185666.504	1.00306043	1340436.283	0.869449527	115.3672983
274	841816.1743	0.998630704	826943.7473	0.866043888	115.3094801
472	1932718.247	0.8609581	2364670.553	0.746812502	115.2843716
259	2252510.923	0.96476799	2713885.481	0.8382621	115.0914481
270	4462500.313	0.826709182	5717928.913	0.71862607	115.0402437
293	10383525.16	0.980566245	13090017.33	0.853441456	114.8955488
261	11867457.86	0.894280073	16278720	0.779633159	114.7052384
342	910225.0588	0.908354809	1304079.75	0.792580955	114.6071961
315	3908746.038	1.204249844	4523253.737	1.053494823	114.3099916
296	3503211.609	0.924465736	4017554.933	0.809716012	114.1716012
299	1848605.521	0.908134297	2820886.164	0.796130537	114.068517
252	2091444.197	0.911941833	2072419.701	0.799519942	114.0611741
75	986399.3829	0.87682815	956369.4023	0.769922602	113.8852331
310	591271.2778	0.864955922	922826.3922	0.759804343	113.8392969
295	3143184.207	0.855559354	3632545.702	0.752534019	113.6904554
495	375650.8481	0.943579724	514464.9405	0.830071218	113.6745503
312	49182075.96	0.919587889	59432664.37	0.809521005	113.5965446
287	2224734.088	0.862060815	2653146.446	0.760778378	113.3130015
					% difference

Ref. Spot	Z-Cy3 Volume	Norm. Vol. Z-Cy3	Cy3 Volume	Norm. Vol. Cy3	(Z-Cy3/Cy3)*100
520	147427.3109	1.036861935	182281.6287	0.917786198	112.9742349
207	1636881.515	0.946830025	1857030.818	0.839518788	112.7824699
323	7709666.911	0.995095362	9070346.315	0.8839585	112.5726335
306	1943806.496	1.041701898	2513237.403	0.92638865	112.4476102
213	91252605.58	0.889155577	132211129.6	0.791116743	112.392461
332	22409595.09	0.944418213	23960708.6	0.841516944	112.2280686
304	882636.0865	0.859285326	1288947.705	0.767326674	111.9842898
324	8488901.009	0.81734764	10796958.51	0.731056908	111.8035588
265	8131307.109	0.848870027	10888955.96	0.759772846	111.7268183
309	1503075.786	0.993461451	2169649.813	0.890492273	111.5631748
331	1793242.48	0.889812285	2903502.64	0.797883458	111.5215858
281	992431.8072	0.972700918	1036291.602	0.87267085	111.4625197
302	2227211.225	1.054900639	2263384.75	0.946934359	111.4016647
360	1862730.145	0.894843419	2122773.722	0.80376645	111.3312727
289	4442805.734	0.896627688	4878807.581	0.806866069	111.1247235
352	1347123.716	1.029529315	1688461.525	0.926773652	111.0874605
282	459677.0906	0.973020169	807278.8352	0.876394344	111.025382
276	3655306.892	0.888311065	5101909.164	0.800106681	111.0240779
343	18937893.91	0.938066375	23062310.51	0.845074043	111.0040455
227	2159725.636	0.915704066	1711795.335	0.825656259	110.9062103
325	857300.8908	0.868454863	1117980.048	0.784920982	110.64233
286	4067927.416	0.920244005	4519899.598	0.831952821	110.6125229
537	26033391.47	0.964257796	31630651.78	0.872007213	110.5791078
351	2404333.131	0.995583138	2581138.418	0.902285894	110.3400978
499	120203.32	0.929310918	91563.57019	0.844848734	109.9973143
277	2315706.038	0.951442656	2625508.118	0.865488567	109.9312795
254	2650876.079	0.850076066	3636904.597	0.775151211	109.6658373
359	1339626.418	0.991613593	1815278.823	0.905922358	109.4590043
284	7340777.696	1.007384338	9570295.041	0.92077015	109.4067111
314	3934938.785	0.92022666	5064751.143	0.843132876	109.143729
109	633716.5934	0.971467764	781564.9602	0.891199048	109.0068224
308	1903916.378	0.90323738	2258000.003	0.828912398	108.9665666
333	7508123.167	1.020806586	8931343.707	0.937211959	108.9195007
322	13722549.1	0.856048446	17424187.93	0.786275868	108.8738038
523	1329473.935	0.954700457	1857298.852	0.880253944	108.4573904
550	387351.4493	1.078182398	403204.7801	0.995886938	108.2635344
285	103086173.8	1.046660415	135515235.9	0.96956559	107.9514811
361	559205.5086	0.999727645	674119.9796	0.927519698	107.785058

328	4427812.855	0.890932508	5439499.799	0.829382581	107.4211743
278	2057516.637	0.905378652	2843264.803	0.843869759	107.2889083
517	296657.0248	1.117123888	298094.6628	1.041546702	107.2562456
348	32152554.3	0.870091106	44296309.74	0.81146761	107.224379
555	1388818.831	0.843516966	1720712.147	0.787298445	107.1406875
338	10006614.93	0.849059752	15656221.06	0.794793665	106.8276949
341	1519651.249	0.896898928	2609711.74	0.840419773	106.7203506
307	352924.2421	0.871974504	389420.1585	0.817988267	106.5998791
519	836778.7584	1.079740247	877953.3411	1.016555054	106.2156194
327	697188.3721	1.091245991	821999.1958	1.027988594	106.1535116
508	2866239.971	0.835726399	3323215.267	0.787624241	106.107247
528	282208.1005	0.988052025	474334.0931	0.93463279	105.7155319
511	897420.2077	1.026565736	1286304.842	0.973386777	105.4632917
300	3712519.31	0.929126347	4266016.205	0.881326895	105.423578
497	247069.0917	0.82299751	217751.7582	0.781606745	105.2955998
490	193597.9771	0.944204839	288531.1752	0.903207437	104.5390904
345	57092556.44	0.935672083	86893179.08	0.895266344	104.5132646
318	425107.7313	1.058169629	480457.0958	1.012568283	104.5035329
329	4093011.985	0.848203367	4290489.312	0.811788296	104.4857842
502	1324322.613	0.87899498	2557726.666	0.842146195	104.3755805
303	1693146.009	0.788750948	2590282.588	0.755859817	104.3514856
320	2234587.862	0.897516165	2912580.818	0.860362282	104.3183998
524	1466551.445	0.963435364	2201907.675	0.928297877	103.7851521
358	1135441.063	0.995099689	1563630.379	0.959019077	103.7622414
473	745292.2481	1.430435871	1300399.282	1.380311281	103.6313976
549	2568885.185	0.941498924	3416846.148	0.912735833	103.1513051
546	420734.4959	0.994888657	698258.0941	0.969879046	102.5786319
548	1378761.111	1.017044003	1877807.799	0.992239446	102.499856
515	1441684.9	0.9946521	1758985.932	0.971028835	102.4328077
264	1522419.988	0.999753718	2513491.198	0.976481762	102.3832453
552	668266.4416	0.977126418	915654.6769	0.954503796	102.3700923
518	11688744.74	0.879997373	16443306.41	0.86040229	102.2774327
336	1573719.323	0.900038441	1998421.927	0.883404154	101.8829758
356	536118.6888	1.006362256	753470.9206	0.988823028	101.773748
222	2017412.951	1.001852424	2771109.874	0.985122653	101.6982425
547	6440890.106	0.984990647	6716326.482	0.972674878	101.2661753
539	6090068.74	0.920828788	10826348.84	0.90985248	101.2063832
566	424904.1119	0.959850199	576692.1955	0.948580913	101.1880152
554	960062.8751	0.91732683	1330094.55	0.906728143	101.1688936
					% difference

Ref. Spot	Z-Cy3 Volume	Norm. Vol. Z-Cy3	Cy3 Volume	Norm. Vol. Cy3	(Z-Cy3/Cy3)*100
565	507276.5207	0.969684962	862545.3815	0.961848805	100.8146973
349	3352811.879	0.817048973	4243230.633	0.811508461	100.6827424
479	2621496.524	1.032858203	4069726.905	1.026127154	100.6559664
551	392571.8947	1.048544382	485229.6364	1.045477847	100.2933141
556	200209.8477	1.102900297	233543.947	1.103499378	99.94571078
561	86105.15417	1.240948287	173335.4199	1.241778022	99.9331817
521	2094784.532	0.936109327	2205246.43	0.939772945	99.61015917
340	2273756.893	0.942107347	2404680.73	0.946440848	99.5421266
347	3320847.459	0.770347355	4858919.589	0.773894744	99.54161865
498	35935577.33	1.123277579	50514350.34	1.135006272	98.96664066
560	781257.6345	1.057306563	929521.2904	1.074344095	98.41414572
545	2441450.814	1.088065723	3654520.548	1.106517151	98.33247701
522	2768130.399	0.866632035	3148663.775	0.884227408	98.01008511
505	111958.3587	0.94808226	132536.6286	0.970573859	97.68264945
339	2843344.796	1.016729281	4199978.775	1.043806048	97.40595806
335	2967129.695	1.051002831	3817017.393	1.080038696	97.31159025
485	1720814.955	1.004029623	2211313.19	1.031926578	97.29661438
354	4709454.933	0.966150266	8321614.972	0.993720009	97.22560246
317	865216.4013	0.861034156	1047554.986	0.887942057	96.96963322
364	2866131.198	1.005593441	4898773.513	1.03842865	96.83799091
326	6085669	0.808897772	8533716.507	0.836085261	96.74823962
526	1676309.921	0.842950013	2247320.611	0.873260218	96.52907523
491	396102.3273	1.062573848	466817.1964	1.102421084	96.38547949
540	14664554.14	0.876087726	20063072.48	0.909535629	96.32252973
553	1314305.519	0.862624891	2137041.953	0.897829525	96.07891778
563	1541000.256	0.875123715	2149638.292	0.911105296	96.05077697
466	846545.095	0.922156256	1459527.27	0.960352949	96.02264012
534	3709189.392	0.938234121	4346339.609	0.977770328	95.95649345
290	2385546.852	0.973273948	3374358	1.015534519	95.83858846
504	1282915.257	1.035868648	1699761.077	1.081283614	95.7999025
559	238586.526	0.797433244	466312.4494	0.832654907	95.76995672
144	664217.2234	1.168266412	1054299.74	1.221775692	95.62036792
288	1680567.234	0.984177852	2664446.466	1.031449432	95.41697559
564	14888932.64	1.008174303	19519800.1	1.05721934	95.36094028
542	31592972.99	0.882928876	43231555.78	0.928221951	95.1204478
330	2177882.473	0.998662709	3179290.635	1.050362485	95.07791104
363	1449312.966	0.854532303	1930686.664	0.902359448	94.69976789
					% difference

Ref. Spot	Z-Cy3 Volume	Norm. Vol. Z-Cy3	Cy3 Volume	Norm. Vol. Cy3	(Z-Cy3/Cy3)*100
301	1597630.677	0.991358666	2392303.602	1.047369064	94.65227684
457	438376.6359	1.136688108	660632.3793	1.206941623	94.17921181
493	3698330.595	0.771822494	6405243.235	0.819721213	94.15670618
350	2152409.221	1.061558767	2675328.161	1.133470683	93.65559979
258	1295057.364	0.923278452	1849542.139	0.998750878	92.44331818
530	388224.7572	1.175758352	636096.4781	1.275774063	92.16038999
357	737635.1366	1.02645179	1417733.099	1.11567696	92.00259809
538	1226106.985	0.934012322	2738074.685	1.030640922	90.62441655
214	372433.4532	1.200928007	704635.9725	1.334300682	90.00430137
492	392862.0546	0.91714922	758100.925	1.036063602	88.52248235
355	2650350.504	0.954227478	3840583.581	1.090405626	87.5112394
255	828534.0453	1.018877755	1598834.894	1.183555687	86.0861695
436	40471.88991	0.991186167	116976.3843	1.161178952	85.36032839
313	532429.4269	0.803829313	973970.6734	0.959892513	83.7415963
316	785740.74	0.796391507	1094670.561	0.954388056	83.44525083
482	71234.3008	0.857460044	111240.5278	1.02825885	83.38951267
238	1391380.235	0.861563818	2103718.748	1.056536935	81.54601981
251	2785774.735	1.127027321	4111551.483	1.392605617	80.92939647
195	2312960.747	0.859853748	3257782.643	1.14050037	75.39267599
212	138560.2959	0.919162254	190128.0031	1.232534899	74.57494749
425	1525228.545	0.644493339	2443581.371	0.887525378	72.61689121

APPENDIX C

Z-Cy5 VS. Cy5 DIGE FLUOR: SPOT VOLUME COMPARISON

					% difference
Ref. Spot	Z-Cy5 Volume	Norm. Vol. Z-Cy5	Cy5 Volume	Norm. Vol. Cy5	(Z-Cy5/Cy5)*100
44	726250.7937	1.798767756	273059.6185	1.073176468	167.6115542
43	4500363.237	3.494237113	1759343.856	2.134813384	163.6788087
14	17634823.42	1.608282377	7448110.268	1.059442539	151.8045875
26	1441924.708	1.602048109	647988.2559	1.061350975	150.9442349
71	3094886.607	1.375737667	1240084.724	0.946276678	145.384294
112	1636144.666	1.170125858	1126406.403	0.820350571	142.6372942
80	12049099.27	1.378495164	5443484.968	0.967803116	142.4354955
85	8303220.134	1.384689169	4195829.307	0.988226026	140.1186704
75	1954078.946	1.2635546	939518.0019	0.906242538	139.4278626
69	3227955.704	1.173853967	1391122.032	0.845054987	138.9085899
131	264832.4251	1.391442657	157972.8629	1.020441139	136.3569739
134	3977634.01	1.226383285	2423301.664	0.912523982	134.3946361
138	697377.2045	1.166715261	471133.1626	0.870646851	134.0055682
154	7009744.541	1.348001104	5223223.121	1.023999054	131.6408545
216	19167231.05	1.281039187	14330862.1	0.975472448	131.3249995
99	1236884.362	1.193254458	803886.4339	0.909646194	131.1778652
117	2410911.739	1.007455304	1463351.524	0.769365192	130.9463067
116	3464145.616	1.144847384	1778793.055	0.879700876	130.1405302
126	4479452.946	1.066098981	2238334.671	0.819953327	130.0194713
203	1674149.787	0.985469388	1013041.923	0.767175577	128.4542181
119	21399814.12	1.26046383	11684768.48	0.982316427	128.3154588
100	20719998.2	1.237014415	9293767.726	0.965650331	128.1016922
406	2376630.325	1.758854698	1208095.462	1.377664159	127.669337
114	2114098.512	1.251105835	1178740.575	0.980743092	127.5671321
437	1234741.118	1.06893181	688710.1099	0.841704846	126.9960385
92	3650721.568	1.124749634	2148477.47	0.887597733	126.7183987
188	2482953.214	1.317705123	1833581.81	1.040909372	126.5917244
123	31164792.4	1.094698553	13775809	0.865759239	126.4437622
249	2792216.278	0.878059081	1083086.25	0.695550049	126.2395256
132	3095670.316	1.153693567	1475320.592	0.915335728	126.0404824
102	2019446.458	1.149129346	1235130.31	0.914356281	125.6763222
82	2208169.452	1.274452799	1149541.034	1.014284684	125.6504035
204	4550743.383	0.993737005	3090581.535	0.792511022	125.3909381
243	231529.9022	0.900942337	158286.5567	0.722055724	124.7746271
201	1264084.464	0.967214866	883494.3206	0.776029078	124.6364207
					% difference

Ref. Spot	Z-Cy5 Volume	Norm. Vol. Z-Cy5	Cy5 Volume	Norm. Vol. Cy5	(Z-Cy5/Cy5)*100
77	1823888.145	1.097480358	998831.9881	0.881787062	124.4609277
232	1786032.589	1.000050246	1536243.52	0.803768249	124.4202228
181	12807116.5	1.178418633	7046579.723	0.947584087	124.3603232
392	2165734.875	1.330864527	1177019.823	1.070854149	124.2806528
157	1103245.646	1.11049105	748259.6044	0.895314001	124.0336964
104	19863835.67	1.209820991	9703449.278	0.976777228	123.8584353
167	1161921.419	1.211012669	729302.1186	0.978210993	123.798718
299	2810983.122	0.99073241	2235941.068	0.809357245	122.4097784
147	16746949.51	1.099255739	9846190.675	0.898338559	122.3654186
172	3280022.461	1.065501588	1589670.444	0.871007514	122.3297814
237	1398751.376	0.934170799	535876.1864	0.764329386	122.2209712
163	8064034.066	1.119148839	4436641.372	0.916827993	122.0674814
478	1285770.487	1.367300854	530786.8198	1.125162029	121.5203516
142	68686673.42	1.058338562	31921560.95	0.877863247	120.5584772
242	1858931.776	1.143152298	1152474.541	0.948273704	120.5508803
186	8563469.777	1.139645795	4360922.478	0.945751375	120.5016271
184	1249295.755	0.977749889	780247.0013	0.813365796	120.2103522
136	3560071.751	1.105746791	2445262.954	0.921726087	119.9647928
245	9033577.214	1.128701846	7145076.817	0.940894676	119.9604882
246	4793255.287	1.175186866	3308823.51	0.981622282	119.7188459
302	3466051.991	1.174348039	1861645.32	0.982529798	119.522893
191	106419100.5	1.089704613	52007467.43	0.914441716	119.166109
162	29058839.05	1.105656537	22209390.27	0.928460772	119.0848952
166	0.880352175	2648061.755	0.73945009	119.0549824	119.0549824
198	2556585.245	1.116556834	1771297.749	0.939144123	118.8908929
84	5835610.892	1.425207983	3263273.65	1.200011445	118.7661992
440	2740879.832	1.406066076	1551425.722	1.18493984	118.6613893
252	3306170.066	1.044892932	1814874.808	0.881915956	118.4798761
206	5232626.906	0.989868303	3683925.647	0.836010649	118.4037911
247	2942777.999	1.069554949	2109479.968	0.903320802	118.4025594
300	6093690.244	1.096617796	3565750.201	0.928115832	118.1552731
224	3424540.929	0.938776417	2418238.4	0.795426239	118.0218066
221	1480635.838	1.069670716	934667.9412	0.906590441	117.9883073
473	960623.4439	1.377505044	875610.0089	1.16798077	117.9390174
139	6250423.402	1.210620711	3517952.787	1.026934981	117.8867926
199	5940284.397	1.040836454	3530779.986	0.882950034	117.8816937
327	1094601.175	1.229590928	660531.2601	1.043400385	117.8445921
					% difference

Ref. Spot	Z-Cy5 Volume	Norm. Vol. Z-Cy5	Cy5 Volume	Norm. Vol. Cy5	(Z-Cy5/Cy5)*100
315	5617432.165	1.273335651	3668491.975	1.08186945	117.6977177
125	4717777.145	1.159703942	4191568.507	0.985966126	117.6210736
143	77132365.64	1.212920051	50475410.94	1.034438108	117.2539992
225	4028097.238	1.073135987	2389540.374	0.916165253	117.1334519
310	865721.4293	0.925201878	754272.3497	0.790405918	117.054017
306	2920808.833	1.136610184	2078367.243	0.971400768	117.0073384
169	7769646.512	1.191120927	4438959.402	1.019674836	116.8138003
256	5556797.151	1.176531199	3906480.856	1.007913613	116.7293688
230	37405081.04	1.150498876	28682899.39	0.987452764	116.5117885
228	3984705.263	1.067675283	3019197.836	0.916674294	116.4726981
185	1744463.177	1.095471488	1268917.324	0.942474837	116.2334998
333	11414252.48	1.113629955	7306044.62	0.958681428	116.1626712
175	3274375.787	1.08338872	2198364.375	0.932916143	116.1292715
342	1301469.294	0.933490752	1041033.575	0.804641409	116.0132628
135	6997676.609	1.055152157	3863201.665	0.909521316	116.0118118
291	4340572.09	1.085003531	3376067.716	0.935597764	115.9690171
113	3843861.385	1.157816583	2936720.408	0.999135381	115.881852
250	1881522.977	1.041374887	1293900.603	0.899263458	115.8030917
273	1935178.185	0.86148232	1406943.943	0.745608278	115.5408739
505	159398.3895	0.972584127	89847.13079	0.84222802	115.4775315
220	16379990.24	1.052588775	9861246.172	0.916007808	114.9104588
197	18134045.12	0.952348474	11042830	0.829793088	114.769391
127	7552794.558	0.973171051	4686997.979	0.848784504	114.6546675
161	7506733.801	1.155492958	4874700.941	1.008299489	114.5981894
207	2724702.44	1.133057052	1725793.17	0.990709139	114.368285
280	2978386.955	1.059171172	2344887.41	0.9284623	114.0779946
259	3585649.646	1.087132776	2434604.93	0.953240913	114.0459627
137	1640717.29	1.03203728	1194555.05	0.905867746	113.9280303
515	2203181.96	1.10031615	1384923.096	0.966119258	113.8903029
211	20394054.59	0.965682447	13539726.55	0.847958452	113.8832267
309	2279056.385	1.085287431	1826012.202	0.953126208	113.8660779
218	13036253.55	1.209111952	9643348.467	1.063110312	113.7334421
150	3625589.243	1.101166951	2417364.235	0.969038489	113.6350065
165	3184168.053	1.117541892	2310311.92	0.983504869	113.6285063
227	3561749.512	1.09796349	1585692.232	0.968695456	113.3445484
183	21905286.53	1.044036149	13840484.08	0.921412581	113.3082151
286	6480664.747	1.057390798	4011828.422	0.933388046	113.2852303
					% difference

Ref. Spot	Z-Cy5 Volume	Norm. Vol. Z-Cy5	Cy5 Volume	Norm. Vol. Cy5	(Z-Cy5/Cy5)*100
190	1949959.378	0.880850296	1483348.714	0.778999869	113.0745114
159	1312342.497	0.993641313	864610.8135	0.879005283	113.0415632
257	5603876.72	1.040356359	3386507.619	0.920583967	113.0104798
194	4431660.763	0.996644262	3449943.086	0.883696225	112.7813194
519	1187672.21	1.072278602	650854.1815	0.950856844	112.7697201
334	1216372.004	0.912564722	829025.7077	0.809270787	112.7638284
294	17903533.29	1.01808662	12196938.93	0.907189999	112.2241891
283	51626671.87	0.993881489	28937024.29	0.886043782	112.1706974
495	543222.6826	0.975566213	427534.2618	0.872952299	111.7548135
205	620751.801	0.992074763	466296.1335	0.887870722	111.736398
284	11979686.06	1.17093977	8610374.113	1.049083696	111.6154769
234	928488.1866	0.950159491	906146.8759	0.852554044	111.4485936
248	11646645.2	0.953035774	8781960.565	0.85592528	111.3456742
521	3264167.07	1.055974355	1796817.735	0.948532764	111.3271354
289	7031501.483	1.021318158	4389868.569	0.918352229	111.2120301
466	1459292.959	1.14333939	1256928.716	1.0281574	111.2027585
168	660514.1694	0.960109232	581692.5555	0.863443451	111.1953806
511	1347570.57	1.114763472	1043102.585	1.00364154	111.0718745
275	64026592.33	1.021256235	38093994.33	0.92067834	110.9243251
282	744146.0363	1.115327052	730177.155	1.006968791	110.7608361
193	1677555.613	1.000952481	1168583.858	0.905362644	110.5581821
277	3730733.531	1.105502326	2396300.6	1.000837647	110.457708
229	22582214.83	1.063179946	13352432.74	0.963241464	110.3752264
304	1383417.001	0.944961212	1140307.741	0.857915534	110.1461828
312	72717728.38	0.984809585	51861495.37	0.894541959	110.0909325
467	774122.9495	0.930628344	621765.097	0.847269944	109.8384701
298	2944926.483	1.048553064	2008858.383	0.956045265	109.6760899
352	1978447.752	1.061142952	1383751.591	0.968998766	109.5092161
524	2201492.307	1.044993472	1823059.4	0.956997974	109.1949514
545	3549841.41	1.161729521	2784963.05	1.064096248	109.1752295
358	1687714.649	1.076987719	1268511.808	0.986963698	109.1213103
210	2588831.137	1.099370283	1985755.117	1.009162142	108.9389145
345	90862288.7	1.048792507	74287744.4	0.965303216	108.6490223
548	2004948.584	1.062647468	1471892.472	0.979062079	108.537292
189	33296076.95	1.054597663	22371902.31	0.972338179	108.4599665
263	9875759.224	1.047352685	6370955.575	0.96599357	108.4223247
261	18834990.93	1.009663807	15387059.38	0.931529921	108.3876947
					% difference

Ref. Spot	Z-Cy5 Volume	Norm. Vol. Z-Cy5	Cy5 Volume	Norm. Vol. Cy5	(Z-Cy5/Cy5)*100
265	13083345.44	0.978467127	10221357.43	0.902797243	108.3817141
332	33093604.44	1.000322098	20801059.37	0.924238137	108.2320733
472	2900933.723	0.914682025	2123289.986	0.8457611	108.1489826
271	19859628.32	1.10303511	11963835.23	1.020905463	108.0447848
223	2211246.254	0.942238939	1578727.741	0.872262312	108.0224293
340	3705311.054	1.111009865	2116299.472	1.029663319	107.9003054
320	3616323.585	1.03400979	2563619.68	0.958820307	107.8418743
499	185379.0521	0.989085617	79795.29289	0.917271468	107.8291054
360	2639846.318	0.901088457	1745376.417	0.835888504	107.8000776
279	6656802.418	1.042874574	4242508.073	0.967527128	107.7876313
331	2687910.82	0.95019585	2533959.152	0.88166866	107.7724425
272	28469487.99	1.030925631	16319784.56	0.956680688	107.7606817
319	6202851.16	0.965292573	3501224.663	0.895840848	107.7526857
517	423758.8968	1.058029003	216271.193	0.982306947	107.7085941
239	24195713.33	1.066465782	16559452.32	0.990509813	107.6683711
523	1910636.995	0.992791598	1548129.178	0.922601513	107.6078442
337	11881080.66	1.031644663	8860579.527	0.959744555	107.491588
490	304128.6544	1.067447029	252739.7435	0.993933639	107.3962071
547	9601687.895	1.056807199	5387672.449	0.984135107	107.3843613
329	6467407.084	0.968104466	3785861.392	0.901957901	107.3336643
202	7977810.652	0.991991909	6110028.685	0.925743787	107.1562048
187	1462794.965	0.996298398	1320533.951	0.930510351	107.0701037
233	11359910.48	0.995986596	9142244.766	0.932186166	106.8441727
231	3332506.707	0.987322143	2583227.43	0.924960925	106.7420382
307	565604.1542	1.001206678	358909.4397	0.938504793	106.6810405
260	16913114.28	1.011909638	12954276.98	0.949861846	106.5322965
276	5863440.797	1.022251975	4847097.134	0.961188659	106.352896
278	3421408.165	1.075787981	2691055.965	1.011531365	106.3524096
215	2603033.452	0.918993198	1830970.924	0.86620497	106.0941959
528	369632.28	0.933142057	352055.6976	0.879712348	106.0735431
270	6968921.186	0.92340961	5480132.252	0.872070036	105.887093
479	4421416.234	1.246037181	3692303.549	1.178919684	105.6931357
323	11547466.65	1.059954302	8127180.849	1.002885327	105.6904785
308	2971272.454	1.010840891	2059087.509	0.956453783	105.6863288
254	4422310.924	1.012376547	3553925.801	0.958750469	105.59333
326	10296398.27	0.968794938	7343885.981	0.918605957	105.4636028
492	641688.7416	1.08122507	609260.6152	1.02533279	105.4511355
					% difference

Ref. Spot	Z-Cy5 Volume	Norm. Vol. Z-Cy5	Cy5 Volume	Norm. Vol. Cy5	(Z-Cy5/Cy5)*100
534	5643891.964	1.041369428	3476169.065	0.988464336	105.352251
281	1556428.239	1.110744568	989464.5284	1.055483494	105.235617
348	48690526.33	0.942235578	38594748.54	0.895406206	105.2299584
325	1302113.41	0.940393023	1005303.742	0.895372873	105.0280895
560	1138989.365	1.121234749	730335.0582	1.067684302	105.0155694
520	201927.6199	0.989072425	147613.4988	0.942259821	104.9681206
508	4326125.98	0.90822239	2873814.926	0.865293255	104.9612238
293	15754509.68	1.069059479	12339657.7	1.019188067	104.8932492
361	808621.2167	1.03659797	567240.4486	0.988526151	104.8629789
317	1446220.658	1.038371783	954905.2297	0.991404761	104.7374215
564	21349577.88	1.053326018	14779437.66	1.007289883	104.5702965
287	3455909.874	0.966769021	2546066.806	0.924803083	104.5378241
359	1915799.005	1.017063789	1536808.817	0.976283139	104.1771335
537	36001404.69	0.95223807	26178260.05	0.914381547	104.1401233
355	4252000.444	1.087530945	2908026.781	1.045139091	104.0560969
338	15351350.48	0.938237584	14027342.82	0.901946279	104.0236659
226	99941753.95	1.060040948	71545259.51	1.020941512	103.829743
328	6862829.917	0.99007693	4976033.323	0.955234762	103.6474979
253	4202281.779	1.292501993	2965713.935	1.247576476	103.6010231
343	28210084.26	0.993652207	20685468.34	0.959881519	103.5182142
555	1946704.096	0.840103826	1399371.196	0.81243546	103.4056079
213	150760166.2	1.059230037	134984404.8	1.02500366	103.3391469
262	3271777.064	1.019017081	1918341.916	0.987649862	103.1759452
552	971496.4949	1.03001579	765288.8396	0.999524144	103.0506163
236	1005681.891	0.993643746	735141.3809	0.964289189	103.0441653
494	925688.209	0.906261824	767770.3585	0.881130914	102.8521198
482	116727.7338	1.028249905	86933.47238	1.006197632	102.1916442
274	1284061.156	1.108149174	813176.3051	1.08532271	102.103196
322	21068075.22	0.944293335	16175731.67	0.925868721	101.9899813
561	113903.3189	1.190460113	130576.3278	1.172524487	101.529659
526	2575487.446	0.947807235	1907300.712	0.934633997	101.4094542
295	4776381.26	0.940021222	3554914.506	0.928141265	101.279973
556	269470.396	1.043422285	173123.6855	1.030725041	101.231875
539	9474395.657	1.003143704	9364741.591	0.991508734	101.1734611
553	2010930.63	0.926973142	1727703.808	0.917107188	101.0757689
530	508313.4892	1.152709592	450309.8648	1.140900244	101.0350903
212	215603.5384	1.150075782	139904.2342	1.138384818	101.0269781
					% difference

Ref. Spot	Z-Cy5 Volume	Norm. Vol. Z-Cy5	Cy5 Volume	Norm. Vol. Cy5	(Z-Cy5/Cy5)*100
347	0.899103867	4411113.681	0.890376992	100.9801327	100.9801327
549	3779218.048	0.989643699	2898904.262	0.980776279	100.9041226
363	2180640.108	0.920480434	1548119.719	0.912578619	100.8658778
554	1405407.829	0.97167962	1124234.739	0.96500957	100.6911899
498	61009637.66	1.315529448	45944221.08	1.308028892	100.5734244
351	3516338.79	1.04159364	2345755.375	1.036181081	100.5223565
518	18207368.56	0.977416772	14716981.48	0.972615901	100.493604
497	396537.4733	0.915789058	201328.769	0.915172526	100.0673679
565	719967.1156	0.993000704	708463.7706	0.99636421	99.66242209
296	5381988.299	1.004954164	3959294.169	1.010422316	99.45882513
566	640736.0539	0.967304469	466215.2491	0.97308629	99.40582642
324	12601287.72	0.869129726	10211886.22	0.875976738	99.21835685
314	6100422.117	1.006568581	4823838.748	1.019479949	98.73353392
559	346756.7724	0.834708515	374312.3858	0.84565077	98.70605505
540	22390909.74	0.951149907	16796905.81	0.964339692	98.63224701
336	2469371.386	1.027641952	1857874.832	1.043536228	98.47688319
341	2338549.408	0.967538464	2396885.73	0.990173777	97.7140061
502	2031502.506	0.95189304	2336366.228	0.980202826	97.11184409
522	4266049.249	0.948377225	2751456.017	0.977588597	97.01189519
538	1827936.654	0.993251969	2199752.393	1.026829108	96.73001683
493	0.878820809	5629036.073	0.909817359	96.59310195	96.59310195
318	660590.7331	1.178079685	457645.6373	1.22017046	96.55041847
550	555074.4847	1.022566127	338347.09	1.063369021	96.16286598
542	46213866.47	0.926982545	35630371.89	0.967389701	95.82307354
563	2160753.255	0.880058745	1717407.11	0.920104032	95.64774354
487	393610.6448	0.818875485	372306.7488	0.864958576	94.67221993
356	791240.4882	1.069406849	685320.4386	1.129686397	94.6640459
551	501822.1863	0.969186371	372111.1773	1.029166371	94.17198205
364	4068909.104	1.014530406	4033172.882	1.079896056	93.94704242
303	0.868255759	2514928.606	0.931035879	93.25696012	93.25696012
313	832207.6783	0.906009142	776874.1138	0.972643522	93.14914677
485	2039449.688	0.867008278	1591196.215	0.934089433	92.81855121
354	5911931.662	0.869355988	6218381.359	0.939966279	92.48799738
316	1203558.196	0.884698776	870400.978	0.961249704	92.03631189
546	525938.3751	0.912098701	564562.4018	0.993153706	91.83862431
491	482020.5781	0.933845757	338673.1296	1.034596011	90.26187484
504	1861742.061	1.077964098	1436070.686	1.198883593	89.91399202
					% difference

Ref. Spot	Z-Cy5 Volume	Norm. Vol. Z-Cy5	Cy5 Volume	Norm. Vol. Cy5	(Z-Cy5/Cy5)*100
290	3775816.886	1.102797946	3234498.705	1.230981777	89.58686206
301	2460616.475	1.093562243	2221782.333	1.231600789	88.7919408
266	150868509.2	1.080292598	132872014.7	1.225883758	88.12357549
285	147868269.7	1.085362134	135888840.2	1.232307669	88.07558058
357	997665.5271	0.988868161	1126930.083	1.126190175	87.80649867
339	4087089.233	1.05053757	3811668.089	1.199682131	87.56799346
238	1790022.797	0.802332092	1443458.631	0.917621531	87.4360578
264	2339378.114	1.097764585	2547213.604	1.258764598	87.20968058
251	3538305.12	1.064786581	2851962.104	1.221414703	87.17649935
330	3148356.816	1.032709949	2843537.654	1.189615994	86.81036186
288	2566037.17	1.080337536	2547861.373	1.24616603	86.69290526
350	2921402.594	1.052150312	2288143.35	1.216829038	86.46656837
349	4555171.299	0.802606911	3827044.256	0.928949232	86.39943748
335	4169418.048	1.066499225	3483463.365	1.244118921	85.72325416
214	424814.5706	0.996891181	484851.7253	1.16425591	85.62474732
457	500850.8247	0.949650295	485439.8139	1.11330811	85.29986317
255	1025178.592	0.909739474	1136583.959	1.079504505	84.27380058
425	0.665493374	1737732.7	0.796717917	83.52935965	83.52935965
222	3071411.823	1.085801549	2903765.699	1.311766703	82.77398304
436	48193.50258	0.873419785	80789.71465	1.056140011	82.69924211
109	982995.427	1.098902849	946731.0433	1.358753564	80.87580253
258	1859566.504	0.952155046	1747761.213	1.198575915	79.44052892
195	2931184.278	0.838791663	2457888.235	1.087120482	77.15719438
144	668930.6778	0.853464293	769111.9465	1.120805517	76.14740293